UNSATURATED SHEAR STRENGTH CHARACTERISTICS AND STRESS STRAIN BEHAVIOR OF EXPANSIVE SOILS OF ADDIS ABABA

A Thesis Submitted to
School of Graduate Studies of Addis Ababa University
In Partial Fulfillment of the Requirement for the Degree of
Master of Science in Civil Engineering

By

HABTOM GEBRE

Advisor

Dr. HADUSH SEGED

November 2010
Addis Ababa, Ethiopia.

ADDIS ABABA UNIVERSITY
SCHOOL OF GRADUATE STUDIES

UNSATURATED SHEAR STRENGTH CHARACTERISTICS AND STRESS STRAIN BEHAVIOR OF EXPANSIVE SOILS OF ADDIS ABABA

By

HABTOM GEBRE

November 2010

Approved by Board of Examiners

Dr. Hadush Seged	_____	_____
Advisor	Signature	Date
Prof. Alemayehu Teferra	_____	_____
External Examiner	Signature	Date
Dr. Messele Haile	_____	_____
Internal Examiner	Signature	Date
Ato Biruk Melaku	_____	_____
Chair-man	Signature	Date

Dedicated to

Desta Maru

Acknowledgements

Above all I am very thankful to Almighty GOD who is always with me in each and every step of my life.

First of all, I would like to express my deepest gratitude to my advisor Dr. Hadush Seged for guiding and supervising my research work. He has been devoting his precious time and providing all necessary relevant literatures and information to carry out the research.

I acknowledge my indebtedness to Prof. Alemayehu Teffera and Dr. Messele Haile for their comments on the progress report and giving advices.

I would like to extend my thanks to my employer, Beza consulting Engineers, for allowing me to pursue M.SC, Degree.

My special thanks also go to my workmates at Megenagna Aratkilo road project for giving their support and encouragement starting from the beginning of the class up to the end.

I also would like to extend my gratitude to my family and friends who in one way or the other had helped me in accomplishing this paper.

I am also grateful for the staffs of Geotechnical testing laboratory of the AAU, especially Ato Yonas Mekonnen, for their support during the research work.

Table of Contents

List of Symbols

u_a	pore air Pressure
u_w	Pore water Pressure
S	matric suction
CD	Consolidated drained
CU	Consolidated undrained
CW	Constant water content
UC	unconfined compression
$\boldsymbol{c'}$	Effective cohesion
$\boldsymbol{\emptyset'}$	Effective internal angle of friction
$\boldsymbol{\emptyset^b}$	Angle indicating the rate of increase in shear strength relative to matric suction
τ	Shear stress
σ	Normal stress
PI	Plasticity index
PL	Plasticity limit
ASTM	American Society for Testing and Materials
AASHTO	American Association of State Highway and Transportation Officials
USCS	Unified Soil Classification System

List of Tables

List of Figures

List of Tables in Appendixes

List of Figures in Appendixes

Abstract

Considerable research work has been done on the shear strength properties of most soils. However, very little information is available on the shear strength characteristics of expansive clays. This work studies the shear strength characteristics of an expansive unsaturated soil found in Addis Ababa. Matric suction is one of the stress state variables that control the shear strength of unsaturated soils. Previous studies on the expansive soils are done using the conventional triaxial machine, which is unable to measure matric suction of the soil. The main aim of this study is to determine the unsaturated shear strength properties and the stress strain behavior of expansive soil found in two locations (Bole and CMC) in Addis Ababa. The shear strength behaviour of unsaturated soil is studied in this work using the consolidated undrained modified triaxial compression equipment with measurements of matric suction during the shearing stage.

In this work, modified consolidated undrained tests were conducted on 12 undisturbed potentialy expansive soil samples collected from Bole and CMC area at 2.5m depth. Six of the tests were on completely saturated samples and the other six on unsaturated samples. Range of values of shear strength parameters (c, $\emptyset'$, and $\emptyset^b$) were obtained from the consolidated undrained test depending on the applied matric suction. According to the outcome of the research, the deviator stress of soils from Bole area ranges from 90.65 kpa to 130.08 kpa for effective consolidation of 250 kpa for matric suction range of 0 Kpa to 75 Kpa. Similarly the soils from CMC area ranges from 54.03 to 93.41 kpa in deviator stress for effective consolidation of 150 kpa and for matric suction range of 0Kpa to 75 Kpa. The result clearly shows that the shear strength of expansive soils tested for unsaturated case is higher than that of saturated soil and the shear strength increases when matric suction increases.

Chapter 1 - Introduction

1.1 General

Expansive soil is a term generally applied to any soil or rock material that has a potential for shrinking or swelling under changing moisture conditions. The degree of expansiveness depends on whether the soil mass contains active clay minerals or not. The most common active clay mineral in expansive soil is montmorillonite (Chen, 1975).

Expansive soil is the major problematic soil in Africa and other parts of the world. Large parts of Ethiopia are covered by black and gray expansive soil (Ayenew, 2004). The expansive clays of Ethiopia are residual, derived from weathering of basic volcanic rocks. In the capital Addis Ababa, it has been noticed that expansive soil covers large part of the city where recent construction are carried out. Most of the structural damage on expansive soil results from the differential rather than the total movement of the foundation soil as a result of swell (Ayenew, 2004).

Expansive soils cause more damage to structures, particularly light buildings and pavements, than any other natural hazard, including earthquakes and floods because of their swell and shrink properties (Nelson and Miller, 1992). Expansive soils are difficult to use in the construction of highways, airfields, and lightweight structures, because such light structure can't exert the necessary counter load to overcome the swelling. Structural crack may occur if the foundations are not adequately designed to withstand the stresses and strains caused by alternate heaving and shrinkage of the foundation soil. Cracks do not only affect the structural safety and aesthetics of the building but also bring about additional financial burden to owners for repair if the structure is to be salvaged at all. Thus, a detailed investigation and research should be carried out on expansive soil to know in more detail the behavior of the soil and make remedial measures that are safe and economical.

The degree of expansiveness of the soils varies from place to place depending upon type of parent material, climate and topography. Amount of clay minerals in the soil, thickness of expansive soil zone, and thickness of the active zone also affect the degree of swell and shrinkage (Chen, 1975).

Types of structures most often affected by swelling soil include foundations and walls of residential and light (one or two story) buildings, highways, canals and reservoir linings, and retaining walls. Lightly loaded (one or two story) buildings, warehouse, residences and pavements are especially vulnerable to damage because these structures are less able to suppress the differential heave of the swelling foundation soil than heavy, multi-storey structures (Ayenew, 2004).

1.2 Background

Expansive soil is known to be widely spread in Addis Ababa. Although the extent and range of distribution of this problematic soil has not been studied thoroughly, the southern, south east and south west part of Addis Ababa areas, where most of recent constructions are being carried out, are covered by expansive soils (Ayenew, 2004). Ethiopia is found in the tropical zone with high evaporation rate, hence, the soil is not found in full saturation stage as the soil found in temperate zone. The behavior of the soil is in partially saturated (unsaturated). Most of the research done on expansive soils is following the saturated soil mechanics concept which is not related to the actual existence of the soil.

1.3 Objective of the study

The objective of this research is to investigate the unsaturated shear strength properties and stress strain behavior of expansive soils of Addis Ababa.

1.4 Scope of the study

The soil profiles of Addis Ababa vary from place to place. Generally, however, the soil profiles can be divided into two major groups, namely expansive soils and non-expansive soils. The expansive soils, popularly known as black cotton soils which are underlain by grey clay soils, are located in the eastern and southern part of Addis Ababa (Ayenew, 2004). Based on intensity of construction activities going on, two test areas where expansive soils are prevalent were selected namely CMC and Bole area, which are found in Bole sub city. Since most of the footings are placed around 2.5m depth, two test pits with a depth of 2.5m were dug in these places.

From the two test pit areas totally twelve undisturbed samples were collected and six conventional triaxial and six modified triaxial compression tests were conducted. Index property test were made on the samples and for samples that show expansiveness, undisturbed samples were collected and shear strength tests were done on unsaturated samples using the modified triaxial machine. The result of this study can serve as a basis for further study of unsaturated expansive clay soil found in the country.

Figure 1.1 Location of the test pits

1.5 Organization of the thesis

This thesis is organized into five chapters. Chapter one presents the general description and major engineering problems associated with expansive soils. The origin, formation, mineralogy and different characteristics of expansive soils and the concept of unsaturated soil mechanics is presented in chapter two. Chapter three present the test that was made on the samples and the results obtained from the tests. Discussion on the results obtained from the tests is given in chapter four. Conclusion and recommendations are given in the last chapter.

Chapter 2 - Literature Review

2.1 Origin of expansive soil

The origin of expansive soil is related to a combination of conditions and processes that results in the formation of clay minerals having a particular chemical and mineralogical make up, which, when in contact with water expands and when it loose moisture it shrink. Variations in the conditions and processes that determine the clay mineralogy include composition of the parent material and degree of physical and chemical weathering to which the materials are subjected (Chen, 1975).

2.1.1 Parent material

The constituents of the parent material during the early and intermediate stages of the weathering process determine the type of clay formed. The nature of the parent material is much more important during these stages than after intense weathering for long periods of time.

The parent materials that can be associated with expansive soils are classified into two groups (Chen, 1975). The first group comprises the basic igneous rocks and the second group comprises the sedimentary rocks that contain montomorillinite as constituents. The basic igneous rocks are comparatively low in silica. Rocks that are rich in metallic base such as pyroxenes, amphiboles, biotite and olivine fall within this category. Such rocks include the gabbros, basalts, and volcanic glass. Shale and clay stones are some of the sedimentary rocks that contain montmorillonite as a constituent (Chen, 1975). Limestone and marbles rich in magnesium can also weather to clay. These constituents of the shales and clay stones contain varying amount of volcanic ash and glass, which are subsequently weathered to montmorillonite (Chen, 1975).

2.1.2 Drainage

Topography has a major influence on drainage characteristics that in turn is known to have major effect on soil mineralogy. Its control over soil properties is particularly strong in tropical environments reflecting the importance of lateral movements of water and soil material.

Gentle slopes, usually less than 3% results in slow movements or stagnation of water to maintain high concentration of calcium ion for the synthesis of montmorillonite.

2.1.3 Climate

Climate is the principal factor governing the rate and type of soil formation. The two important components of climate are the amount and distribution of precipitation and temperature. The temperature variable is adequately represented by mean annual temperature. According to Van Hoff's principle, the velocity of chemical reaction increases by a factor of 2 or 3 for every 10^0c rise of temperature. The two main rainfall parameters most widely available are the mean annual rainfall and length of the dry season. The amount of distribution of precipitation affects the availability of moisture and the relative humidity of the soil atmosphere; it influences the concentration or chemical activity of solutions in the system. Warm climate with altering dry and wet seasons is favourable for the formation of montmorillonite.

2.2 Distribution of expansive soils

Potentially expansive soils can be found almost anywhere in the world. In the underdeveloped nations, many of the expansive soil problems may not have been recognized because of less intensity of construction (Chen, 1975). It is to be expected that more expansive soil regions related problems would be reported each year as the amount of construction increases. Expansive soils are in abundance where the annual evaporation exceeds the precipitation. The problem of expansive soil is wide spread throughout the world.

2.3 Mineralogical characteristics

Two units are involved in the atomic structure of most clay minerals. One unit consists of closely packed oxygen or hydroxyl in which aluminum (Al), iron (Fe) or magnesium (Mg) atoms are embedded in octahedral coordination. They are equidistant from six oxygen or hydroxyls. When aluminum is present, only two-third of the possible positions are filled to balance the structure, which gives the gibbsite structure and has the formula $Al_2(OH)_6$. When magnesium is present, all the positions are filled to balance the structure and have the formula $Mg_3(OH)_6$ (Grim, 1962).

The second unit is built of silica tetrahedrons. In each tetrahedron, silicon atom is equidistant from the four oxygen or hydroxyls if needed to balance the structure, arranged in the form of tetrahedron with the silicon atom at the centre. The silica tetrahedral groups are arranged to form a hexagonal network, which is repeated indefinitely to form a sheet of the composition

$Si_4O_6(OH)_4$. The tetrahedrons are arranged so that the tips of all of them point in the same direction, and the bases of all tetrahedrons are in the same plane (Grim, 1962).

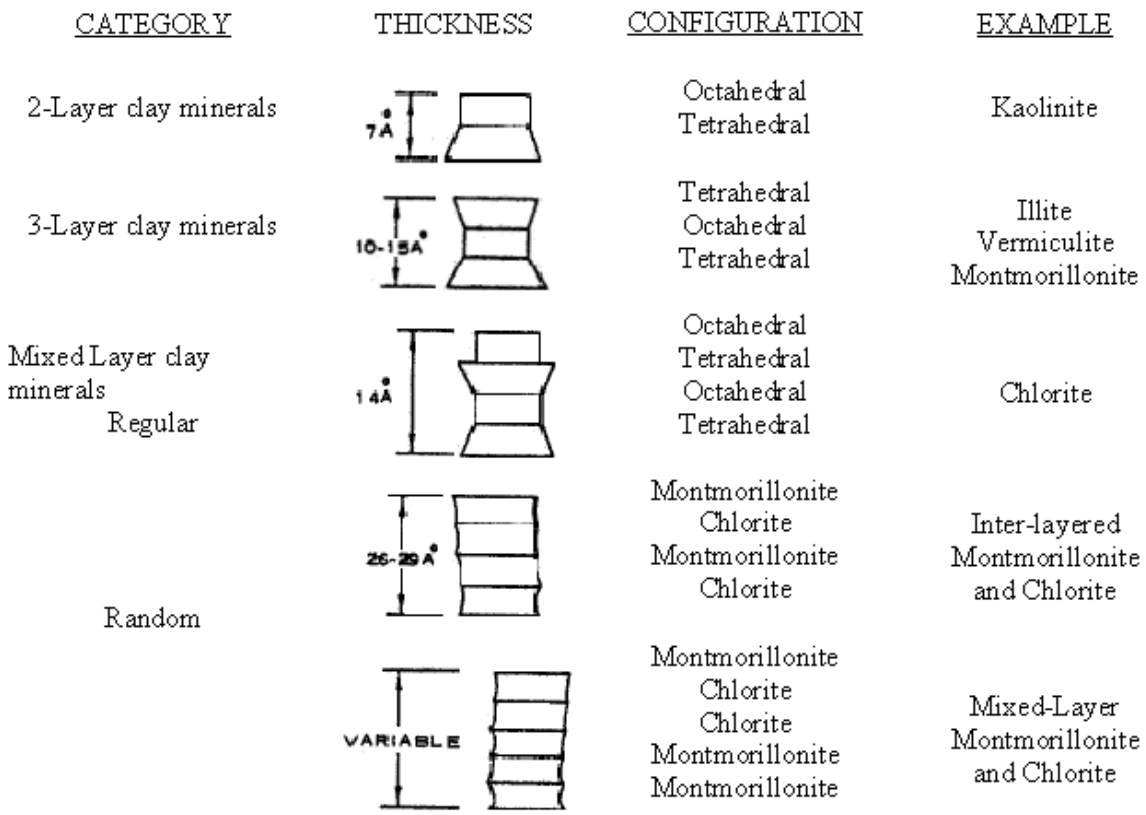

Figure 2.1 Typical structural configeration of clay minerals (Grim, 1962).

The above mineralogical structures lead to the formation of different types of clay minerals, namely kaolinite, halloysite, montmorillonite, illite, etc. But the most common minerals found in clay soils are grouped as kaolinite, illite and montmorillonite (Grim, 1962). They are essential hydrous aluminium silicates. Since clay minerals are products of chemical weathering of rocks, both climate, which determines weathering, and the parent rock, influence the type of mineral found.

Montmorillonite, the principal clay mineral of expansive soil is made up of identical units of alumina octahedral sheets between two silica tetrahedral sheets (Grim, 1962). These sheets are bound rather loosely and are very unstable in water. Water molecules easily insert themselves between the sheets and this is the cause for the highly expansive nature of clays containing this mineral group.

2.4 Mechanics of swelling

2.4.1 General

Swelling in expansive soils will take place if there is change in the environment. Environmental change can consist of pressure release due to excavation and volume increase because of the introduction of moisture. By far the most important element for swelling is the effect of water on expansive soils. With the introduction of water volumetric expansion takes place. If pressure is applied to prevent expansion, the pressure required to maintain the initial volume is the swelling pressure (Chen, 1975).

2.4.2 Moisture transfer

The pattern of moisture migration depends on the geological formation, climatic condition, topographic features, soil types, and ground water level. The most common method of moisture transfer is by gravity. The seepage of surface water, precipitation, and snow melting into the soil are common examples. Moisture migration can occur in all direction. Moisture migration can be caused by different reasons. Fractures and fissures, shrinkage cracks, capillary force, vapor transfer, thermal gradients, etc are some of the sources that cause moisture migration and swelling on expansive soils (Chen, 1975).

2.4.3 Moisture equilibrium

In natural ground, the moisture content of the partially saturated soil is in general equilibrium with the applied stress, the forces due to evaporation and transpiration at ground surface and the capillary forces. When building or pavement covers the area, the evaporation and transpiration forces are eliminated and a new set of equilibrium is established. The new equilibrium requires the flow of moisture compatible with the new condition. The force causing the moisture change or flow is termed as soil suction (Chen, 1975).

2.4.4 Depth of moisture fluctuation

In covered area, there is no gain or loss of moisture to the atmosphere and the moisture content of the soil decreases with depth as shown in curve 1 of Figure 2.2. In uncovered natural

conditions, evaporation and transpiration causes loss of moisture content in the soil near the ground surface. Hence, the moisture content will increase with depth. However, the influence of evaporation decreases with depth and at some depth, H_d, the moisture content equilibrium remains the same as the covered condition. The value of H_d depends on climatic condition, type of soil and location of the water table. This depth represents the total thickness of the material, which has a potential to expand because of change of moisture content. The maximum depth of H_d is equal to the depth of the water table, and the minimum depth is equal to the depth of the seasonal moisture contents fluctuation, H_s. During wet months with heavier precipitation and higher humidity, the moisture content of near surface soil increases and the moisture profile represented by curve 2 alters its shape to curve 3 (Chen, 1975).

The watering of lawns, planting of trees and shrubs, discharge of roof drains, formation of drainage channels and swales, and the possibility of utility line leakage will all increase the value of H_s. When areas are covered by structures such as buildings, pavements, sidewalks or aprons, evaporation is blocked or partially retarded. The moisture content beneath the covered area increases due to gravitational migration, capillary action, vapor, and liquid thermal transfer and, in the course of several years, the depth of seasonal moisture content fluctuation H_s can approach to the depth of desiccation H_d (Chen, 1975).

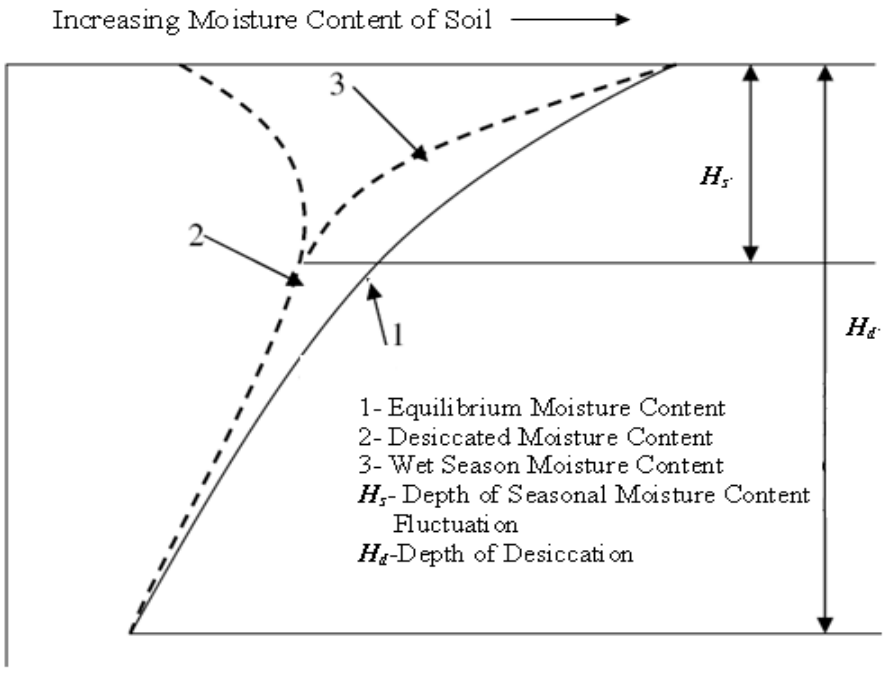

Figure 2.2 Moisture content variations with depth below ground surface (Chen, 1975).

2.5 Unsaturated soil mechanics

2.5.1 General

The general field of soil Mechanics can be subdivided in to portion dealing with saturated soils and that portion dealing with unsaturated soils (Figure 2.3). The differentiation between saturated and unsaturated soils becomes necessary due to the basic differences in their nature and engineering behavior. An unsaturated soil has more than two phases i.e. the solid, water, air and that of the air-water interface or the contractile skin (Fredlund, 1993). Moreover, the pore water pressure is negative relative to the pore air pressure. Any soil near the ground surface, present in a relatively dry environment, will be subjected to negative pore-water pressures and possible desaturation.

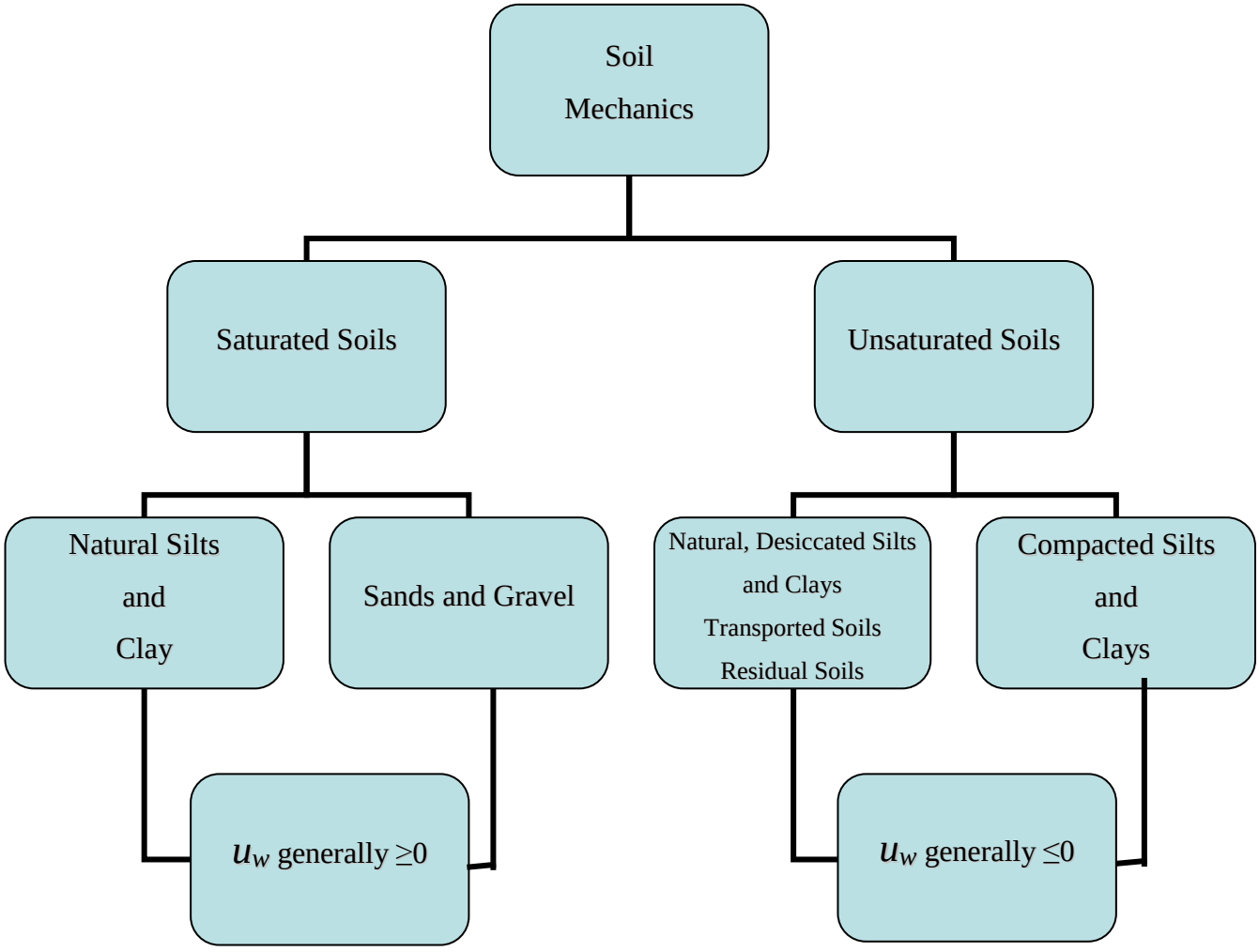

Figure 2.3 Categories of soil mechanics (Fredlund, 1993).

2.5.2 Need for unsaturated soil mechanics

The classical soil mechanics had focused primarily on saturated soil mechanics problem and that present the information relevant to the geotechnical engineering on soils located below the ground water table. While some projects extend well below the groundwater table, many projects remain in the zone above the groundwater table. There was a need to present information relevant to geotechnical engineering on soils located above the ground water table. Soils above the groundwater table are generally unsaturated and have negative pore water pressures (Fredlund, 1993). For example, engineers place building foundations in the zone above the groundwater table to make the construction easy and to be economical. Whenever possible, the geotechnical engineer will attempt to do the design such that construction can remain in the unsaturated zone. In addition to shallow foundations, retaining walls and cuts in slopes are generally designed such that they remain above the water table. Over the past decades, much of the engineering design associated with soils above the water table has remained relatively empirical. At the same time, engineering designs involving soil below the water table have utilized the effective stress analyses in advanced practical designs. The construction of earth dams, highway embankments and airport runways all make use of remolded soils that are unsaturated. In addition, tests on many soils show that they exist under unsaturated conditions. Therefore, unsaturated soil is very important and it has gained increasing attention in many countries (Fredlund, 1993).

Soil mechanics for unsaturated soils also shows how problems with “real-world” flux boundary conditions can be addressed. It is the environment or the climate above the ground surface that is related to the changes in soil suction below the ground surface. These changes in soil suction, in turn, become the trigger mechanism for slope instability and volume change (Fredlund, 1993). The geotechnical engineer understands these mechanisms since the infrastructure for civilization are developed at the boundary between the atmosphere and the ground surface. Changes in the boundary conditions affect the pore water pressures in the soil.

Soils located above the water table have negative pore water pressures. The soils are desaturated due to excessive evaporation and evapotranspiration. Climatic changes highly influence the water content of the soil in the proximity of the ground surface (Fredlund, 1993). Upon wetting,

the pore water pressures increase, tending toward positive values. As a result, changes occur in the volume and shear strength of the soil. Many soils exhibit extreme swelling or expansion when wetted. Other soils are known for their significant loss of shear strength upon wetting. Changes in the negative pore water pressures associated with heavy rainfalls are the cause of numerous slope failures. Reductions in the bearing capacity and resilient modulus of soils are also associated with increases in the pore water pressures (Fredlund, 1993). These phenomena indicate the important role that negative pore water pressures play in controlling the mechanical behaviour of unsaturated soils. The type of problem involving negative pore water pressures that has received the most attention is that of swelling or expansive clays.

2.5.3 Phase system in unsaturated soils

An unsaturated soil is a mixture of several phases. The unsaturated soil behavior (i.e., from both mechanical and seepage standpoints) are highly dependent on the relative fractions of its phases. It has commonly been referred as a three-phase system composed of solids (soil particles), water, and air (Lambe, 1979). However, more recently, the realization of the important role of the air-water interface (i.e. the contractile skin) has warranted its inclusion as an additional phase, when considering certain physical mechanisms (Fredlund, 1993). It is advantageous to recognize unsaturated soil as a four-phase system when performing a stress analysis on an element (Fredlund, 1993).

When the air phase is continuous, the contractile skin interacts with the soil particles and provides an influence on the mechanical behavior of the soil. Understanding of the of basic properties of the soil particles, water, air, and contractile skin is important to establish the number of phases comprising soil which has an influence on how the stress state of a mixture is defined.

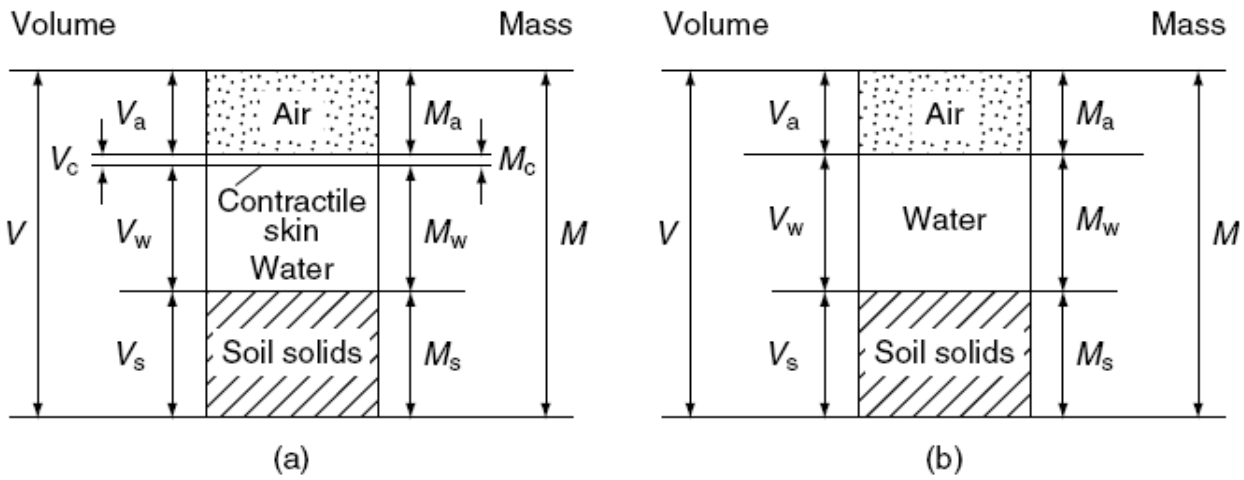

Figure 2.4 Rigors and simplified phase diagrams for an unsaturated soil. (a) Rigorous four phase unsaturated soil system, (b) simplified three-phase diagram (Fredlund, 1993).

2.6 Stress state variables in soils

The mechanical behavior of a soil (i.e., the volume change and shear strength behavior) can be described in terms of the state of stress in the soil. The state of stress in a soil consists of certain combinations of stress variables that can be referred to as stress state variables. These variables should be independent of the physical properties of the soil. The number of stress state variables required for the description of the stress state of a soil depends primarily upon the number of phases involved (Fredlund, 1993).

2.6.1 Stress state variables for an unsaturated soil

Many researchers around the world recognized the importance of soil suction in describing the mechanical behavior of an unsaturated soil. This fact led to the inclusion of the negative pore-water pressure in a single-valued effective stress equation for unsaturated soils. However, later on three independent normal stresses state variables are extracted from the equilibrium equations for the soil structure. These are $(\sigma - u_a)$, $(u_a - u_w)$ and (u_a) that govern the equilibrium of the soil structure and the contractile skin (Fredlund, 1993).

However, unlike saturated soils, the mechanical behavior of unsaturated soils depends on two independent stress-state variables. These variables are the stress tensor, $(\sigma - u_a)$, which is referred to as net normal stress, and the difference between the pore air pressure, u_a, and pore water

pressure, u_w, which is referred to as matric suction (u_a - u_w) (Fredlund, 1993). These combinations appear to be the most satisfactory for use in engineering practice (Fredlund, 1993). The stress variables, u_a, can be eliminated when the soil particles and the water are assumed to be incompressible. Therefore, the $(\sigma - u_a)$ and $(u_a - u_w)$ are referred to as the stress state variables for an unsaturated soil.

The complete form of the stress state for an unsaturated soil in terms of two independent stress tensors is represented in a matrix form as shown below (Fredlund, 1993):

$$\begin{bmatrix} \sigma_x - u_a & \tau_{yx} & \tau_{zx} \\ \tau_{xy} & \sigma_y - u_a & \tau_{zy} \\ \tau_{xz} & \tau_{yz} & \sigma_z - u_a \end{bmatrix} \quad [2.1]$$

and

$$\begin{bmatrix} u_a - u_w & 0 & 0 \\ 0 & u_a - u_w & 0 \\ 0 & 0 & u_a - u_w \end{bmatrix} \quad [2.2]$$

The difference between the pore air pressure (u_a) and the pore water pressure (u_w), which is referred to as the soil matric suction $(u_a - u_w)$, is the quantity that can be used to characterize the effect of moisture on soil (Fredlund, 1993).

2.6.2 Stress state variable for saturated soils

Saturated soil can be viewed as a special case of an unsaturated soil when the degree of saturation approaches 100% (Fredlund, 1993). Then, the four phases in an unsaturated soil reduce to two phases for a saturated soil (i.e., soil particles and water). The stress tensor for a saturated soil indicates that the difference between the total stress and the pore water pressure forms a stress state variable. This stress state variable, $(\sigma - u_w)$, is commonly referred to as

effective stress (Terzaghi 1936). The effective stress law is essential stress state variable, which is required to describe the mechanical behavior of a saturated soil.

$$\sigma' = \sigma - u_w \qquad [2.3]$$

Where: σ' = effective normal stress

σ = total normal stress

u_w = pore water pressure

The volume change process and the shear strength characteristics of saturated soil are both controlled by the effective stress. The complete form of the stress state for saturated soil in terms of stress tensors is represented in a matrix form as shown below (Fredlund, 1993).

$$\begin{bmatrix} \sigma_x - u_w & \tau_{yx} & \tau_{zx} \\ \tau_{xy} & \sigma_y - u_w & \tau_{zy} \\ \tau_{xz} & \tau_{yz} & \sigma_z - u_w \end{bmatrix} \qquad [2.4]$$

2.7 Shear strength theory

2.7.1 General

Many geotechnical problems such as bearing capacity, lateral earth pressures, and slope stability are related to the shear strength of a soil. The shear strength of a soil can be related to the stress state in the soil. The stress state variable used for saturated soils is the effective normal stress $(\sigma - u_w)$ where as the effective normal stress $(\sigma - u_a)$ and the matric suction $(u_a - u_w)$ are used as stress state variables for unsaturated soils (Fredlund, 1993).

The shear strength of saturated soil is described using the Mohr-coulomb failure criterion and the effective stress concept (Terzaghi, 1936).

$$\tau_{ff} = c' + (\sigma_f - u_w)_f \tan\phi' \qquad [2.5]$$

Where τ_{ff} = shear stress on the failure plane at failure

c' = effective cohesion, which is the shear strength intercept when the effective normal stress is equal to zero.

$(\sigma_f - u_w)_f$ = effective normal stress on the failure plane at failure

σ_{ff} = total normal stress on the failure plane at failure

u_{wf} = pore-water pressure at failure

$\emptyset'$ = effective angle of internal friction

The above equation defines a line as shown in Figure 2.5. The line is commonly referred to as a failure envelope. The envelope represents possible combinations of shear stress and effective normal stress on the failure plane at failure (Fredlund, 1993).

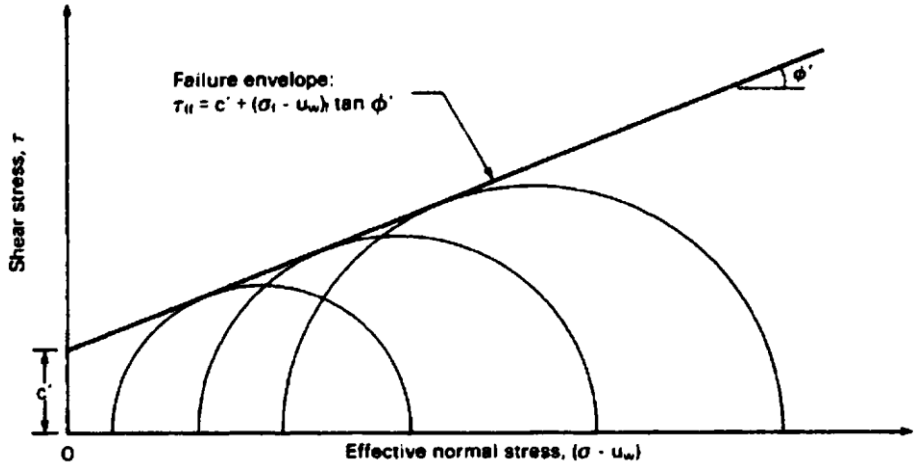

Figure 2.5 Mohr-coulomb failure envelope for a saturated soil (Freduland, 1993).

The failure envelope for a saturated soil is obtained by plotting a series of Mohr circles corresponding to failure conditions on two-dimensional plot, as shown in Figure 2.5. The line tangent to the Mohr circles is known as the failure envelope as described by the above equation.

In case of unsaturated soil, the Mohr circles corresponding to failure conditions can be plotted in a three-dimensional manner as illustrated in Figure 2.6 (Fredlund, 1993). The three-dimensional plot has the shear stress, τ, as the ordinate and the two stress state variables, $(\sigma - u_a)$ and $(u_a - u_w)$ as abscissas. The frontal plane represents a saturated soil when the matric suction becomes zero. On the frontal plane, the $(\sigma - u_a)$ axis reverts to the $(\sigma - u_w)$ axis since the pore air and the pore water equals at full saturation stage (Fredlund, 1993).

The Mohr circles for unsaturated soils are plotted with respect to the net normal stress axis, $(\sigma - u_a)$, in the same manner as the Mohr circles plotted for saturated soils with respect to the

effective stress axis,(σ-u_w). However, the location of the Mohr circles plotted in the third dimension is a function of the matric suction (Figure 2.6). The surface tangent to the Mohr circles at failure is referred to as the extended Mohr-coulomb failure envelope for unsaturated soils. The extended Mohr-coulomb failure envelope defines the shear strength for unsaturated soils (Fredlund 1993). The shear strength equation for unsaturated soils can be expressed as,

$$\tau_{ff} = c' + (u_a - u_w)_f \tan \phi^b + (\sigma_f - u_a)_f \tan \phi' \qquad [2.6]$$

Where τ_{ff} = shear stress on the failure plane at failure

c' = intercept of the "extended "Mohr-Coulomb failure envelope on the shear stress axis where the net normal stress and the matric suction at failure are equal to zero.

$(\sigma_f$-$u_a)_f$ = net normal stress state on the failure plane at failure.

u_{af} = pore air pressure on the failure plane at failure.

ϕ' =angle of internal friction associated with the net normal stress state variable,$(\sigma_f$-$u_a)_f$

$(u_a$-$u_w)_f$ = matric suction on the failure plane at failure.

ϕ^b = angle indicating the rate of increase in shear strength relative to the matric suction.

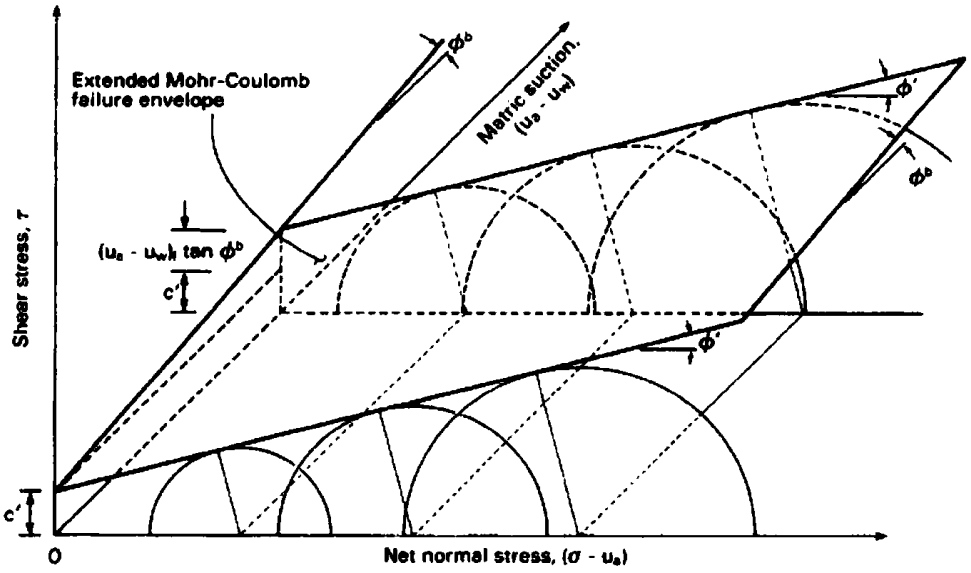

Figure 2.6 Extended Mohr coulomb failure envelope for unsaturated soils (Freduland 1993).

Comparison of the equations 2.5 & 2.6 reveals that the shear strength equation for an unsaturated soil is an extension of the shear strength equation for saturated soils (Freduland 1993).

2.7.2 Tests on shear strength of unsaturated soils

To know the shear strength of unsaturated soils, the parameters u_a, u_w, and σ have to be determined. These parameters can be obtained in the laboratory using either the modified triaxial compression test machine or the modified direct shear test machine.

2.7.2.1 Triaxial tests on unsaturated soils

The triaxial test is the most commonly used method for determining the shear strength of soils in the laboratory. The test is usually performed on a cylindrical soil specimen enclosed in a rubber membrane placed in the triaxial cell. The cell is filled with water then it is pressurized in order to apply confining pressure. The soil specimen can then be subjected to an axial stress through the loading ram in contact with the top of the specimen (Freduland 1993). There are various triaxial test procedures which are used for testing unsaturated soils based on the drainage conditions adhered to during the first and second stages of the triaxial test (Freduland 1993). The methods are usually given a two word designation or abbreviated to a two-letter symbol .The designations are

1) consolidated undrained CU test
2) constant water content test or CW test
3) consolidated drained or CD test
4) undrainded test ,and
5) unconfined compression or UC test

In the above designation the first letter represents the drainage condition prior to shear, while the second letter refers to the drainage condition during shear. In this section the consolidated undrained test is discussed, all others are discussed in Appendix-A.

2.7.2.1.1 Consolidated undrained test

The consolidated undrained or CU uses the test condition where the soil specimen is consolidated first then sheared, with pore air and pore water under undrained conditions (Fredlund 1993). The consolidation procedure is similar to the consolidated drained test. After the consolidation stage, the soil specimen is sheared by increasing the deviator stress $(\sigma_1-\sigma_3)$,

until failure is reached. The drainage valves for both the pore air and the pore water pressures remains closed (under undrained conditions) during shear. Excess pore air and pore water pressures are developed during undrained loading. The pore air and pore water pressures should be measured during the shearing process. The net confining pressure, (σ_3-u_a), and the matric suction, (u_a-u_w), are altered throughout the test due to the changing pore air and pore water pressures. At failure, the magnitude of the net major and minor principal stresses and the matric suction are a function of the pore pressures (Fredlund 1993).

A typical stress path for a consolidated undrained test is illustrated in Figure 2.7. The stress state at the end of consolidation is represented by point *A* where the net confining pressure is (σ_3-u_a) and the matric suction is (u_a-u_w). Shearing causes stress state to move from point *A* to point *B*, along stress path *AB*. The stress state at failure is represented by stress point *B*, corresponding to a different net confining pressure and matric suction from those associated with stress point *A*. As indicated in the drawing, the pore air pressure is assumed to increase continuously during shear. This causes the net confining pressure to decrease [i.e. $(\sigma_3-u_a)_f < (\sigma_3-u_a)$]. The matric suction is also assumed to decrease continuously [i.e. $(u_a-u_w)_f < (u_a-u_w)$]. The failure envelope is tangent to Mohr circle at failure (e.g. at stress point *C*) and inclined at an angle of ϕ^b with respect to the (σ_3-u_a) axis. The failure envelope intersects the shear strength verses (u_a-u_w) plane at a cohesion intercept, *c*. The intersection line joining the cohesion intercepts produced by tests at different matric suctions gives the angle, ϕ^b (Fredlund, 1993).

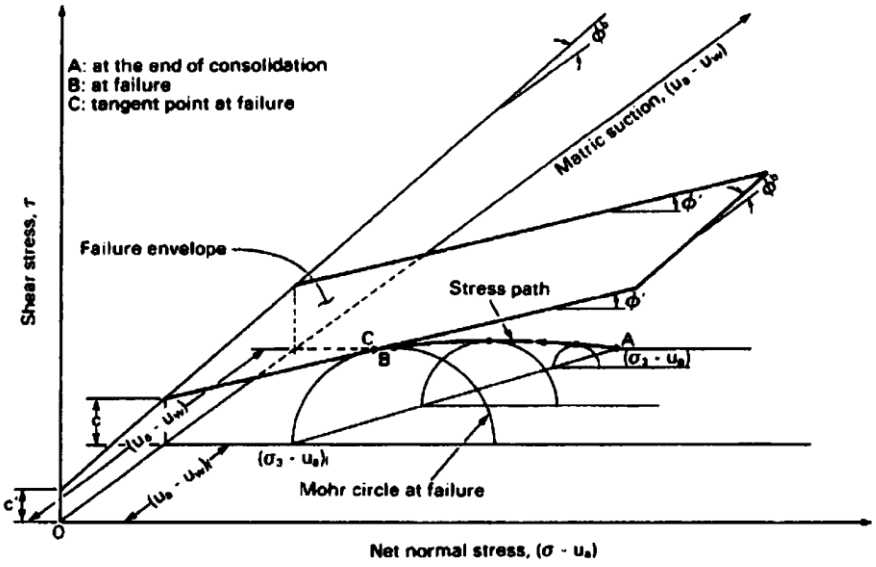

Figure 2.7 Typical stress path followed during consolidated undrained test (Fredlund, 1993).

Chapter 3 – Materials and Methods

3.1 General

Soil samples collected from the test pits, dug in Bole and CMC areas are tested in the laboratory to determine index property, soil classification and shear strength parameters. The various tests done on the samples are shown in the next sections.

3.2 Index property test

To determine the properties of the soil samples collected from the field, index property test is conducted in the laboratory and the results are summarized in table 3.1. Data's used for the determinations of index properties and the grain size distribution of the soils are tabulated from table A-1 to table A-4 and from figure A-6 to figure A-10 of appendix A. The natural moisture content ranges from 40.70% to 44.73% for samples from Bole area and from 44.01% to 53.02% for samples from CMC area. The moisture content of the samples is tabulated in table A-5 of appendix A.

Table 3.1 Atterberg limit, free swell, and specific gravity test results of samples

Location	Depth of Sampling(m)	Liquid limit (%)	Plastic limit (%)	Plastic index (%)	Free swell (%)	Specific gravity
Bole	2.5	99.75	43.82	55.93	170	2.63
CMC	2.5	77.60	44.30	33.30	160	2.65

3.3 Soil classification

Soil classification is an important aspect to know the characteristic of the soil under interest. According to AASHTO classification methods, the soil of the study area falls in the region of *A-2-7* and *A-7-5* (Figure A-10 of appendix A).This means the soil under interest is plastic clay which has a high volume change capacity between wet and dry states.

3.4 Shear strength tests

3.4.1 General

Many geotechnical problems such as bearing capacity, lateral earth pressures and slope stability are related to the shear strength of a soil. The shear strength of a soil is related to the stress state in the soils. The stress state variables to be used for unsaturated soils are the effective normal stress $(\sigma - u_a)$ and the matric suction $(u_a - u_w)$. Therefore, in order to attain a reliable test result of unsaturated soils, the specimen required to be tested with the equipment, which allows the measurement of matric suction (Fredlund, 1993).

The conventional triaxial equipment requires modification prior to their use for testing of unsaturated soils. Several factors related to the nature of unsaturated soil must be considered in modifying the equipment. The presence of air and water in the pores of the soil causes the testing procedure more complex than those required for testing of saturated soils. The modification must accommodate the independent measurement or control of the pore air and pore water pressures.
Most of the time difficulties arise in testing unsaturated soils with negative pore water pressures approaching -1atm (i.e. zero absolute pressure). Water in the measuring system may start to cavitate when the water pressure approaches -1atm (-101.3Kpa gauge). As cavitation occurs, the measuring system becomes filled with water then, water from the measuring system is forced in to the soil and make readings from the pore water pressure transducer unreliable. In addition, if any drainage occurs from an unsaturated sample we will have air in our measuring system, making readings from the volume change transducer unreliable. This problem can be overcome by a technique known as axis translation technique (Fredlund, 1993).

Axis translation technique is commonly used in the laboratory testing of unsaturated soils in order to prevent having to measure pore water pressure less than absolute zero. The procedure involves the translation of the origin of reference for the pore water pressure from standard atmospheric conditions to the final air pressure in the chamber (Hilf, 1956). As a result, the water pressure in the measuring system does not become highly negative, and the problem of cavitation is prevented.

The use of the axis translation technique requires the control of the pore air pressure and the control or measurements of pore water pressure. In a triaxial cell, the pore air pressure is usually controlled through a coarse corundum disk placed on top of the soil sample. The porewater pressure is controlled through a saturated high air entry ceramic disk sealed to the pedestal of the triaxial cell. The high air entry disk is a porous ceramic disk that allows the passage of water but prevents the flow of free air. Continuity between the water in the soil and the water in the ceramic disk is necessary in order to establish the matric suction correctly. The matric suction in the soil specimen must not exceed the air entry value of the ceramic disk (Fredlund, 1993).

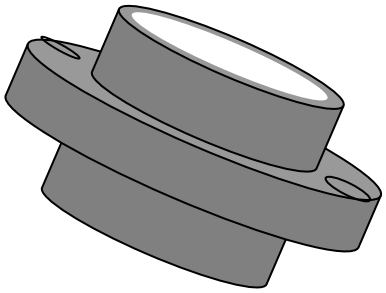

Figure 3.1 High air entry disk used in modified triaxial machine.

The modified triaxial equipment, which has been used for this research work, allows the independent measurement of the pore air and the pore water pressure with the help of specially designed high air entry disk, which allows the passage of water only. The equipment has got volume measuring units for the measurement of the amount of water entering and out of the sample, load cell for measuring the amount of load, pore water pressure and pore air pressure transducers for measuring the pore water and pore air pressures respectively. Each of the measuring unit are connected to the 16-channel data logger and calibrated the data logger in turn connected to PC where the appropriate software has been installed.

Figure 3.2 Modified triaxial machine

3.4.2 Testing procedures

3.4.2.1 Sample preparation

Undisturbed soil samples are collected from the field in 100 mm diameter sampling tubes from a test pit dug to a depth of 2.5m. From this tube, the test specimen having dimension of 70mm diameter and 140mm height was prepared for unsaturated test. To take out the required dimension of soil sample, the sample extractor having dimension of 70mm diameter and 140mm height is pushed into the large size sampling tube, the soil with the sampler tube has been taken out and finally the soil sample with the required dimension extruded from the sampler tube with another sample extractor.

3.4.2.2 Mounting of sample in to the modified triaxial machine

The first step is to remove the entrapped air in the lines by opening the volume change units and allowing de-aired water to pass through until no more bubbles seen comes out from the system. Moreover, by opening the back pressure line the high air-entry disk is allowed to be saturated. Then the sample is placed on the pre-saturated high air-entry disk. After that, it is covered with a rubber membrane and then the loading cap and the coarse porous disk are placed on the top of the specimen and finally after putting O-rings on the rubber membrane the cell placed on its

proper place and filled with water. The installed sample looks like as indicated on appendix B. The assemblage of the modified triaxial equipment is shown in figure 3.3.

3.4.2.3 Testing

From the types of triaxial tests, it is advantageous to test the soil samples by the consolidated undrained test to reduce the time of testing and to determine the total stress and effective stress. Generally, it is also used to test the shear strength for foundations on clay soils, since during the period of construction only a small amount of consolidation will have taken place and consequently the moisture content will have undergone little change (Murthy, 2003). In this thesis, the tests are done using the consolidated undrained test methods. For consolidated undrained triaxial test the following stages has been followed.

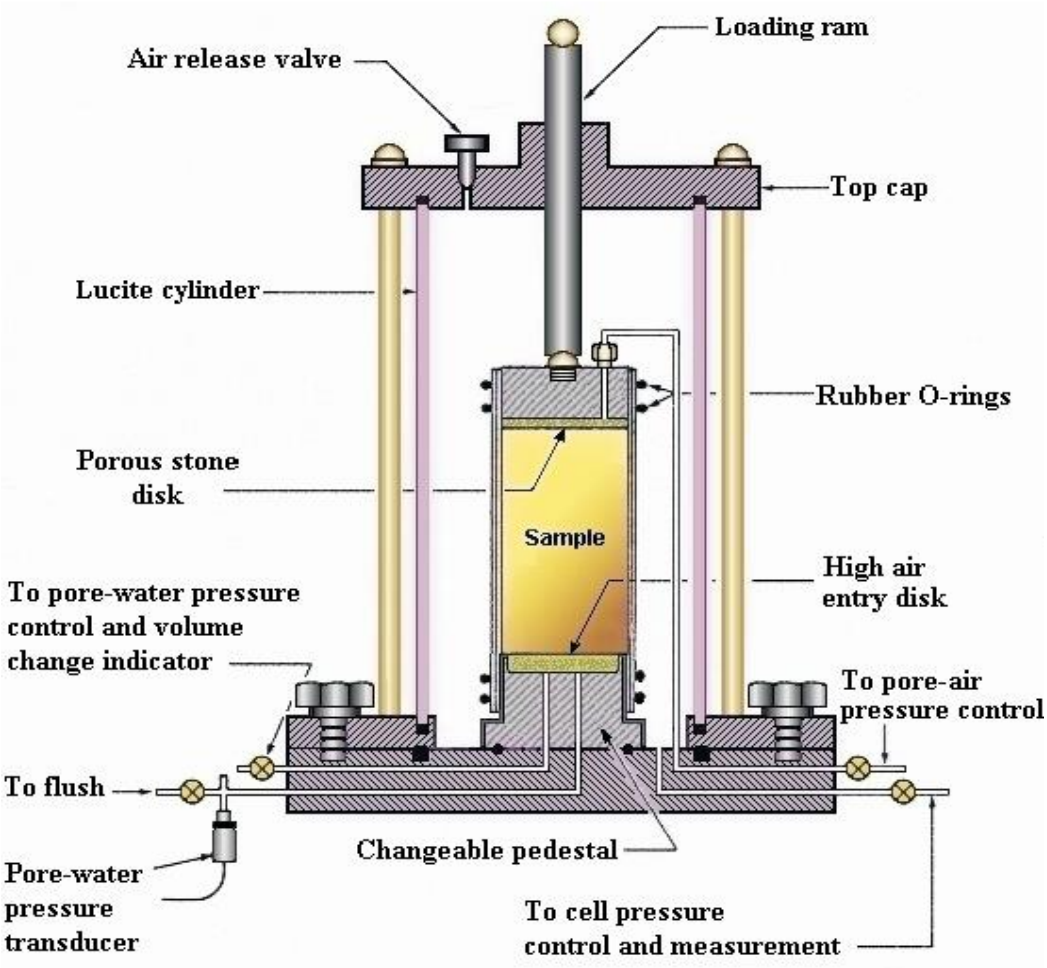

Figure 3.3 Modified triaxial equipment for testing unsaturated soils (Fredlund, 1993).

i) Saturation Stage

The objective of the saturation stage is to ensure that all the voids are filled with water without producing undesirable prestressing of the specimen or allowing the soil to swell. Saturation is commonly achieved by incrementally increasing the pore-water pressure, u_w. At the same time, the confining pressure, σ_3, is increased incrementally in order to maintain a constant effective stress, (σ_3 - u_w), in the specimen. As a result, the pore air pressure increases and the pore air volume decreases by compression and dissolution into the pore water. The simultaneous pore-water and confining pressure increases are referred to as a "backpressuring the soil specimen."

Backpressure technique

The predetermined cell pressure and backpressure were applied at several stages keeping the difference between the two values to 10 kpa until saturation is achieved. The cell pressure should always be larger than the backpressure, so that the effective stress is positive. Saturation of the sample is ensured when the pore water pressure increment divided by the backpressure increment parameter *B* which is given by a relation

$$B = \frac{\delta u}{\delta \sigma}$$

(Where δu-change in pore water and $\delta \sigma$-change in stress) is equal to or greater than 0.95.

Table 3.2 Saturation stage for consolidated undrained triaxial test

Saturation Method	Back Pressure Increments	Cell Increments	50,100,150,200,250,300 kpa
		Back Increments	40,90,140,190,240 kpa
Final B Value		≥0.95	

ii) Consolidation stage

The consolidation stage follows immediately after the saturation stage. Consolidation of the specimen for these tests is isotropic. The objective of the consolidation stage is to bring the specimen to the state of effective stress and matric suction required for carrying out the compression test.

Consolidation procedure

After completion of the saturation stage, the back pressure valve remains closed and the final pore water pressure and volume-change readings are recorded. The consolidation procedure shall be as follows:

A) Increase the pressure *(σ_3)* in the cell pressure line and adjust the back pressure if necessary

B) Adjust the pore air pressure to the value which is the sum of the required matric suction and the pore water pressure at the end of the saturation stage by opening the pore air line.

C) Record the pore pressure when a steady value *(u_i)* (in kpa) is reached.

D) Record the reading of the volume-change indicator. At a convenient moment (zero time), start the consolidation stage by opening the back pressure valve.

E) Record the readings of the volume-change indicator at suitable intervals of time.

F) Allow consolidation to continue until there is no further significant volume change.

G) When consolidation is complete, record the reading of the volume-change indicator, and calculate the total change in volume *(ΔVc)* during the consolidation stage. Record the pore pressure u_c (in kpa) and proceed to the compression stage.

iii) Shearing stage

After the consolidation stage, the samples were axially loaded in compression keeping the cell pressure constant. All the tests were performed under a strain-controlled condition.

Shearing procedure

A) After finishing consolidation, close drainage valves so that the test will be undrained.

B) The loading piston would be lowered to just touch the top of loading cap.

C) A constant shearing strain rate is applied. In this thesis, a constant 0.08 mm/min strain rate was used (based on BS 1990 part 8 calculation procedure).

D) The sample is then sheared by pressing the switches of motor, logger, and computer with closing the drainage valve.

E) The changes in displacement, pore water pressure, pore air pressure and the load are measured automatically.

The test is stopped when one of the following criteria has been clearly identified.

a) Maximum deviator stress;

b) Maximum effective principal stress ratio;

c) Constant shear stress and constant pore pressure

3.4.3 Results obtained from consolidated undrained triaxial test

In order to meet the objective of this thesis, a series of consolidated undrained triaxial tests for unsaturated and saturated case were carried out on expansive soil samples collected from Bole and CMC areas, in which the deviatoric stress-Axial strain results are shown in the figures 3.5 - 3.6 . The conditions that are used in the test are tabulated in table 3.3.

Table 3.3 Test parameters used for consolidated undrained test (for unsaturated and saturated soil case)

Test pit	Sample Number	Effective Consolidation Pressure(Kpa)	Matric suction, *S* (Kpa)
CMC area	C-1	150	0
	C-2	200	0
	C-3	250	0
	C-4	150	25
	C-5	150	50
	C-6	150	75
Bole area	B-1	150	0
	B-2	200	0
	B-3	250	0
	B-4	250	25
	B-5	250	50
	B-6	250	75

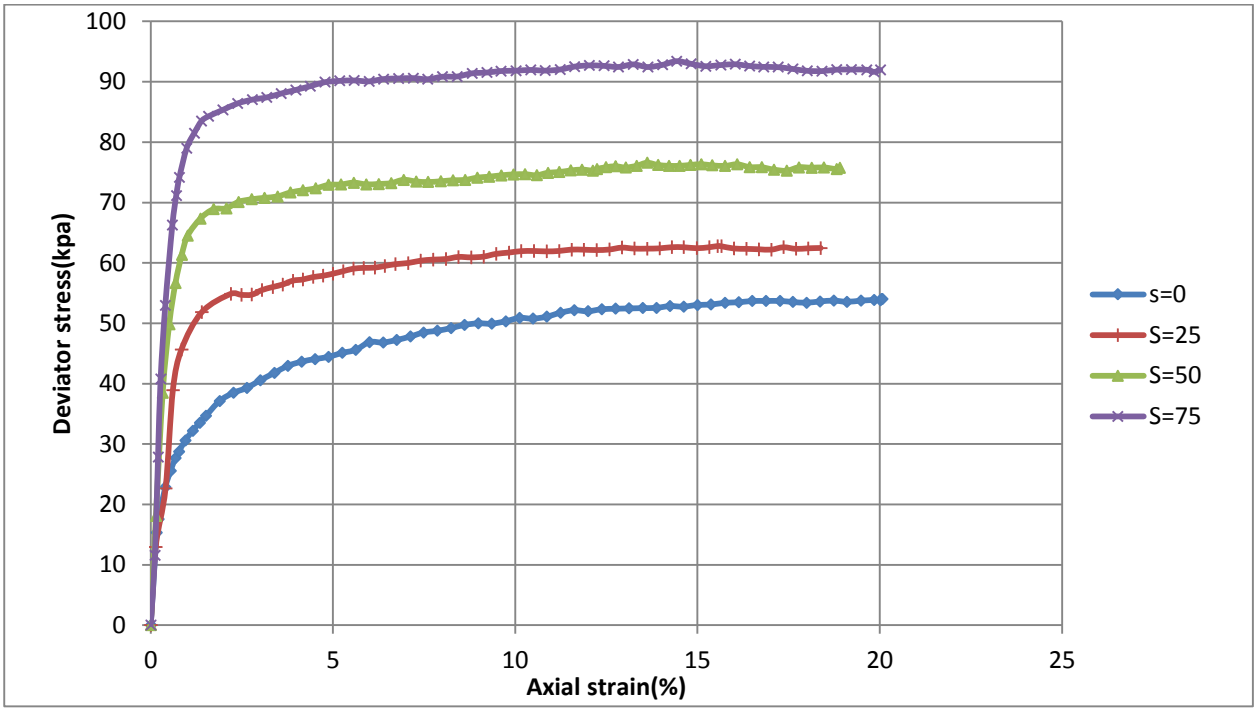

Figure 3.4 Deviator stress Vs Axial Strain for effective consolidation stress of 150 Kpa and different matric suction (sample from CMC area).

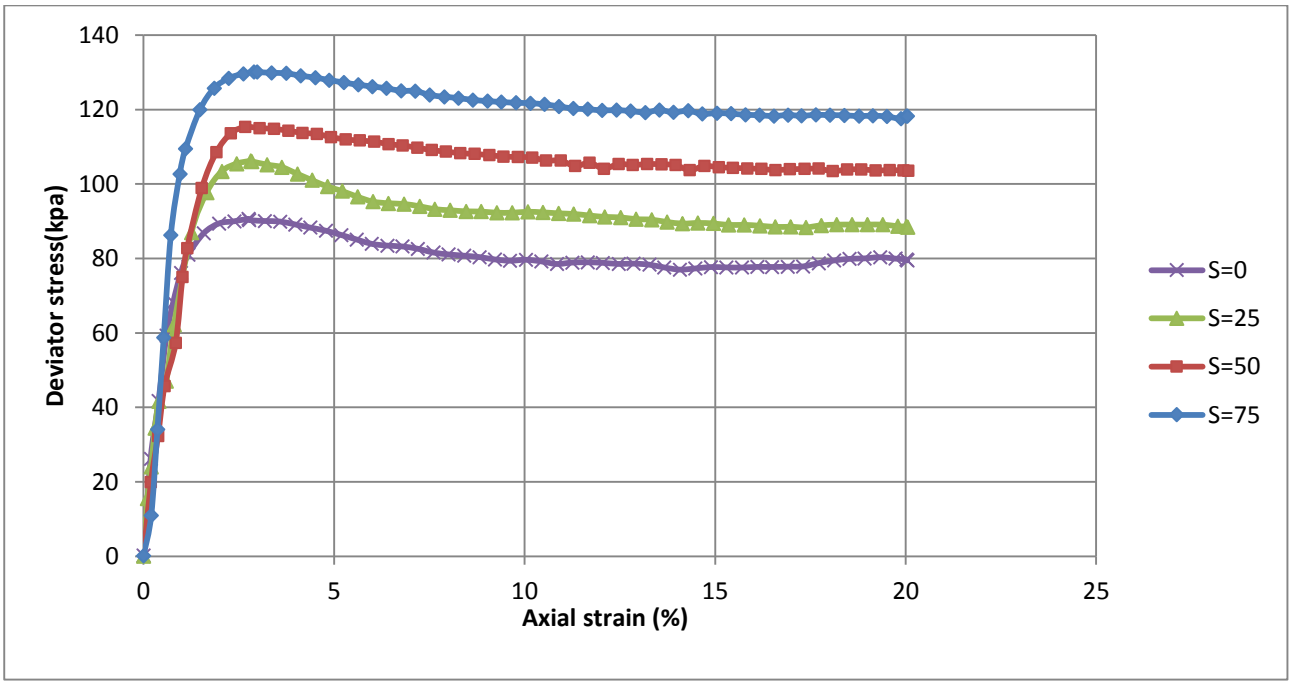

Figure 3.5 Deviator stress Vs Axial Strain for effective consolidation stress of 250 Kpa and different matric suction (sample from Bole area).

For the analysis of the ϕ^b parameter, which is a function of matric suction of the soil, the following procedures have been followed.

1. Mohr circle for the net normal stress has been drawn for maximum deviator stress obtained from triaxial test carried out on saturated soil sample. Then, a best tangent line for the three circles has been drawn to obtain the ***c'*** and ϕ' values of the soil.
2. Mohr circle under the effect of the same net confining pressure, at various matric suctions is drawn for the maximum deviator stress.
3. By drawing a tangent line parallel to the one obtained for saturated soil to the Mohr circles drawn for unsaturated case, the value of cohesion where the failure line intersects the shear stress axis has been taken.
4. Plotting the values of shear stress obtained from step 3, on the graph shear stress versus matric suction axis, the value of ϕ^b is obtained from the best fitting line.

The parameters, which are used to draw figures 3.6 to 3.9, are tabulated in table A-6 and A-7 in appendix A and the results obtained from the figures are summarized in table 3.4.

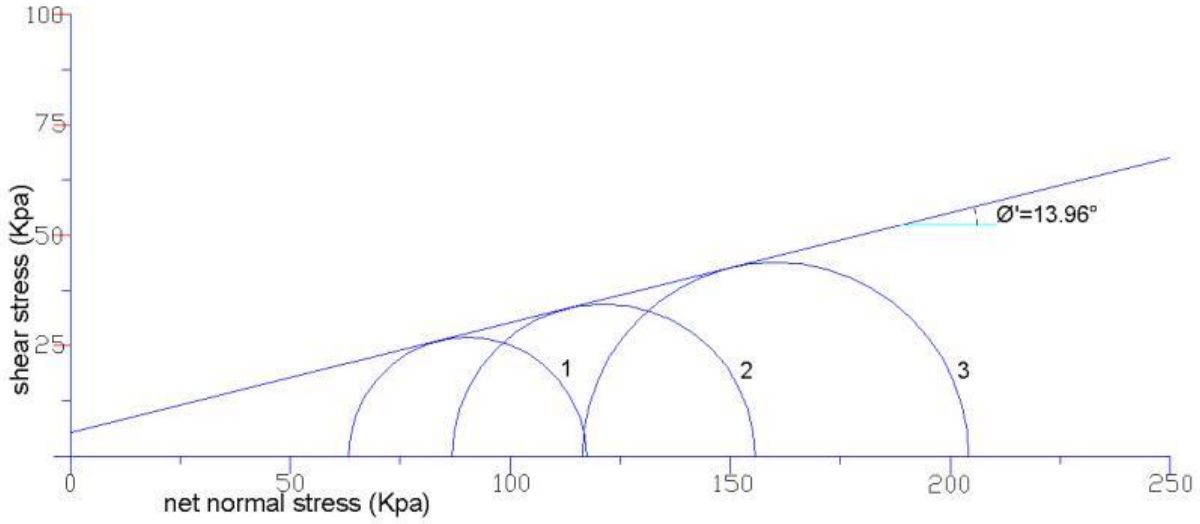

Figure 3.6 Mohr circle for saturated soil under the effect of ($\sigma_{3\,(1)}$ = 150, $\sigma_{3\,(2)}$ =200 and $\sigma_{3\,(3)}$ =250 Kpa) effective consolidation pressure (sample from CMC area).

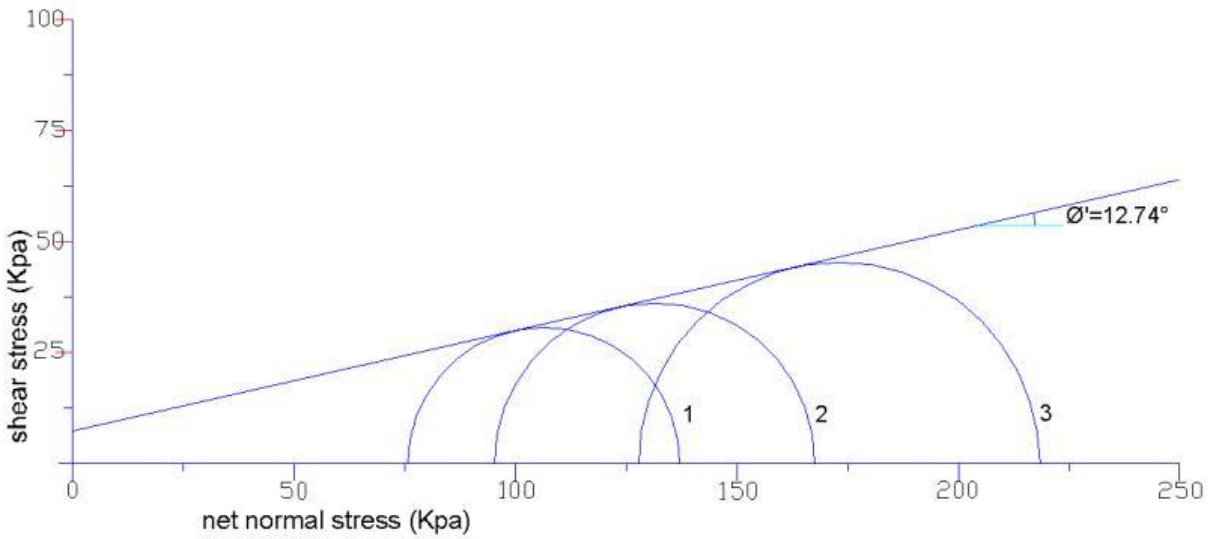

Figure 3.7 Mohr circle for saturated soil under the effect of ($\sigma_{3\,(1)}$ = 150, $\sigma_{3\,(2)}$ =200 and $\sigma_{3\,(3)}$ =250 Kpa) effective consolidation pressure (sample from Bole area).

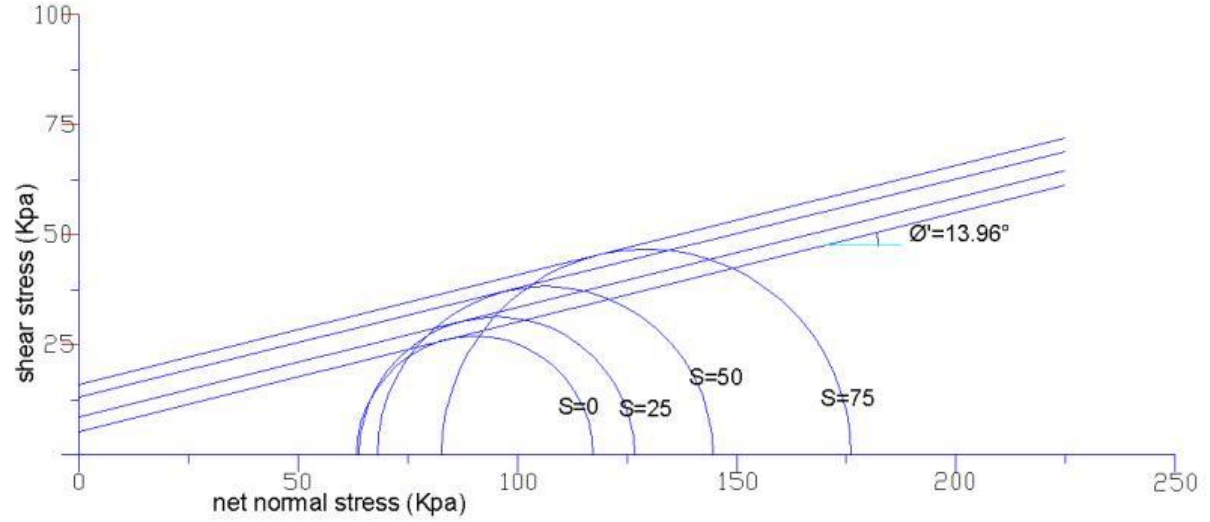

(a)

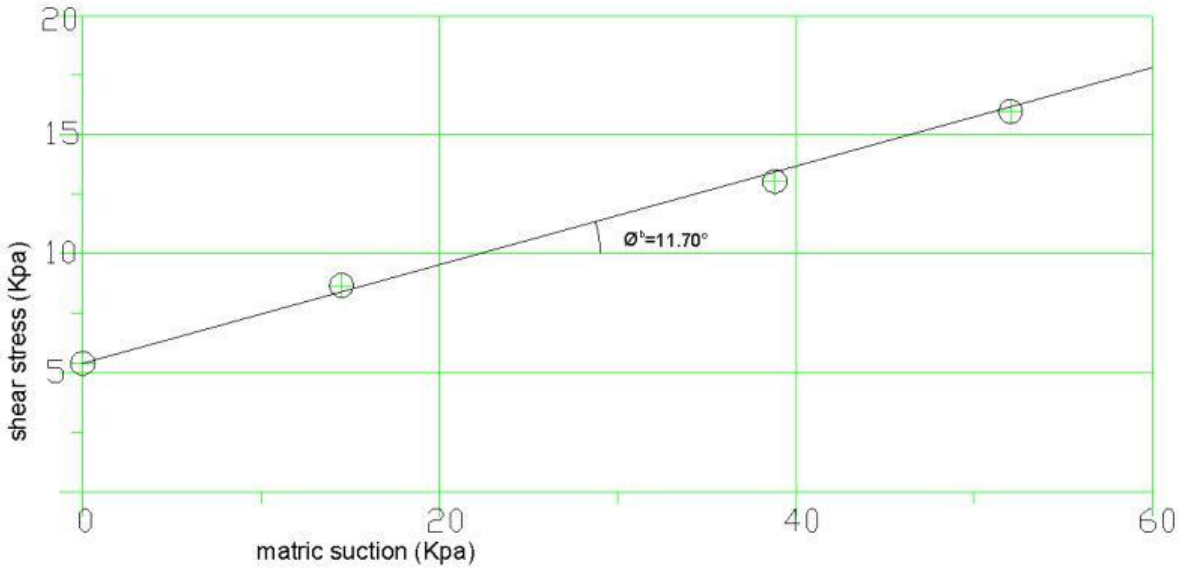

(b)

Figure 3.8 Two-dimensional presentation of failure envelope for samples from CMC area, (a) failure envelope projected on the shear stress versus net normal stress plane, (b) intersection line between the failure envelope and the shear stress versus matric suction plane.

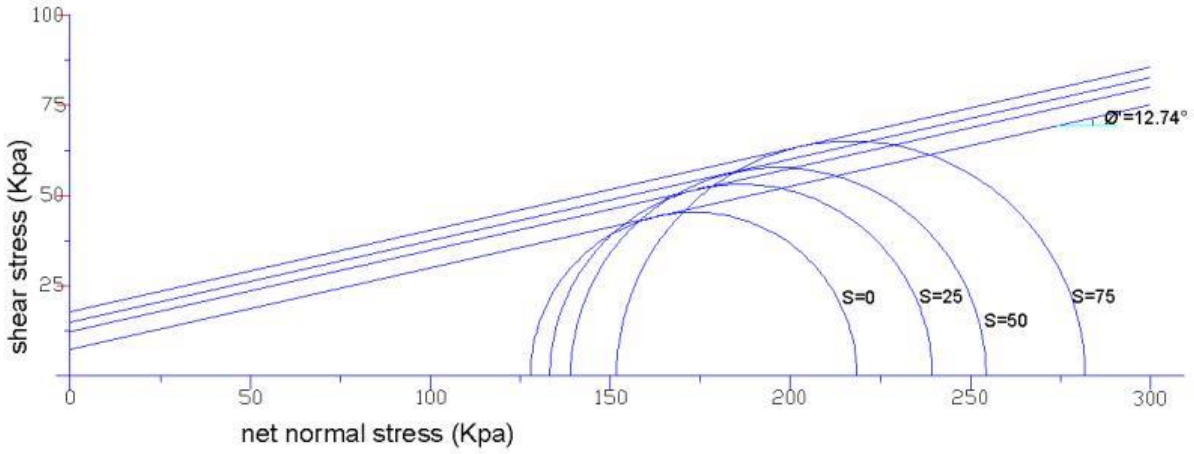

(a)

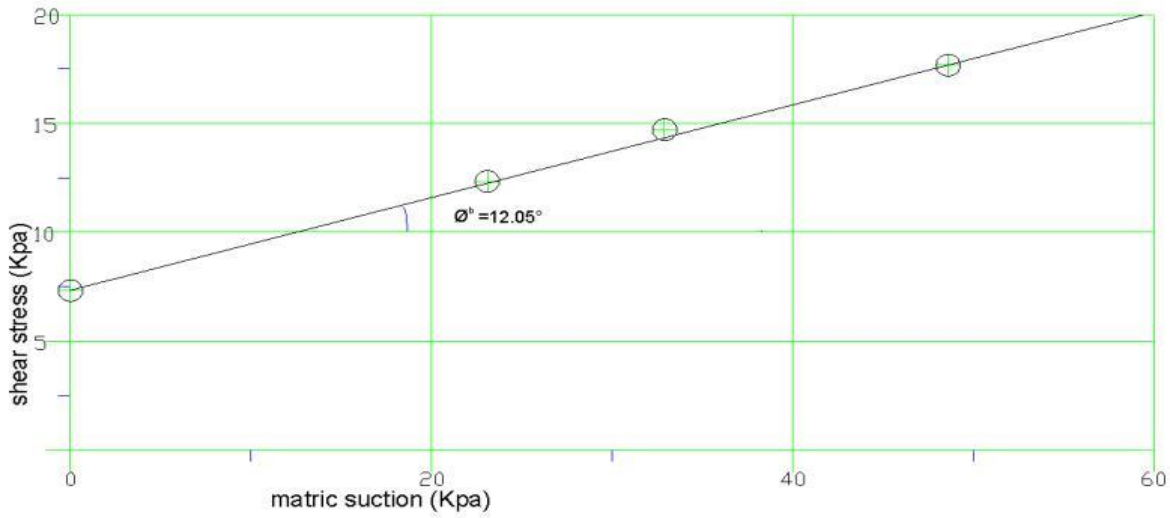

(b)

Figure 3.9 Two-dimensional presentation of failure envelope for samples from Bole area. (a) Failure envelope projected on the shear stress versus net normal stress plane. (b) intersection line between the failure envelope and the shear stress versus matric suction plane.

Table 3.4 Summary of the results obtained for the shear strength parameters.

Test pit	Sample no.	Effective consolidation pressure(Kpa)	C' (Kpa) (for S=0)	C (Kpa)	Matric suction, S (Kpa)	$\emptyset'$(deg.) (for S=0)	$\emptyset^b$(deg.)
Bole area	B-4	250	7.32	12.334	23.1	12.74	12.257
	B-5	250		14.703	32.9		13.561
	B-6	250		17.67	48.6		10.703
CMC area	C-4	150	5.39	8.671	14.5	13.96	12.746
	C-5	150		13.035	38.8		10.172
	C-6	150		15.97	52		12.529

Chapter 4 – Results and discussions

1. As clearly seen from both deviator stress versus axial strain diagrams and table 4.1, at the same effective confining pressure the stress strain diagram of unsaturated soil sample is higher than that of saturated soil sample.
2. More over the values increases when the matric suction of the soil increases. This is because as air enters the pores, a contractile skin begins to form around the points of contact between the particles. The capillary action arising from the suction around the contractile skin increases the normal forces at the inter-particle contacts. This additional normal force will enhance the surface tension and cohesion at the inter-particle contacts. As a result, the unsaturated soil exhibits more strength than that of saturated soil.

Table 4.1 Comparison of failure deviator stress for saturated and unsaturated case

Test pit	Soil sample	Effective consolidation pressure(Kpa)	Deviator Failure stress(Kpa)
CMC area	Saturated soil sample	150	54.033
	Matric suction 25 Kpa		62.79
	Matric suction 50 Kpa		76.586
	Matric suction 75 Kpa		93.41
Bole area	Saturated soil sample	250	90.648
	Matric suction 25 Kpa		106.21
	Matric suction50 Kpa		115.38
	Matric suction 75 Kpa		130.08

3. The failure envelope for saturated soils is represented on two-dimensional plots (Figure 3.6 & 3.7). But the shear strength of unsaturated soils are dependent on the two stress state parameters (i.e. the normal stress and the matric suction axis) as a result of this the failure envelope for Bole area and CMC area has been drawn on three dimensional plots.

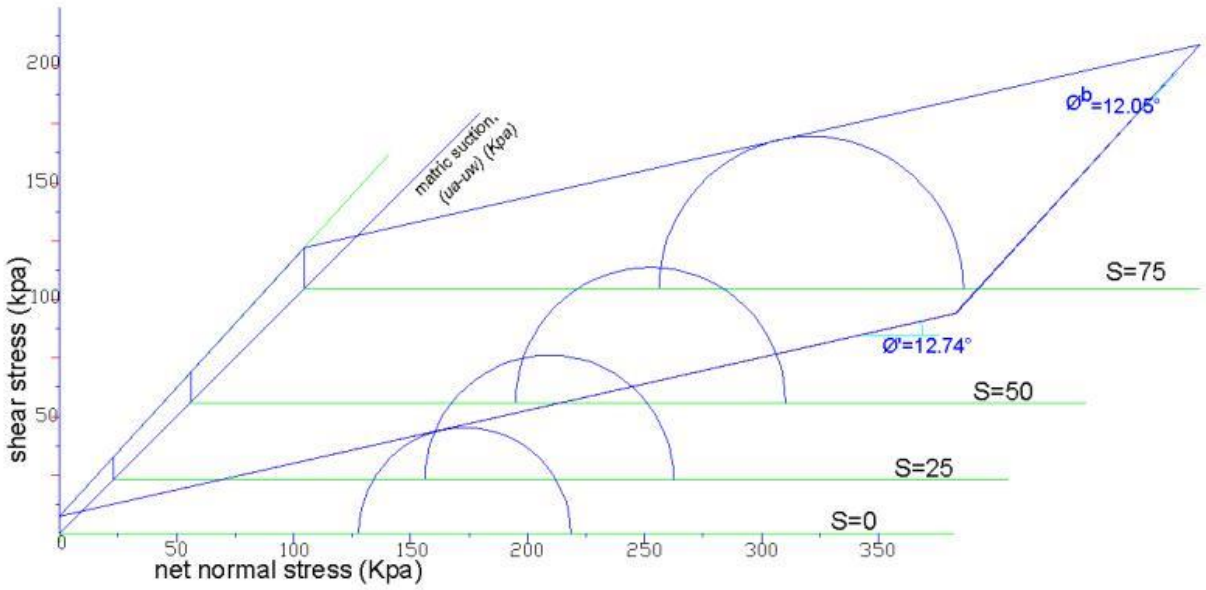

Figure 4.1 Failure envelopes for unsaturated soil from Bole area.

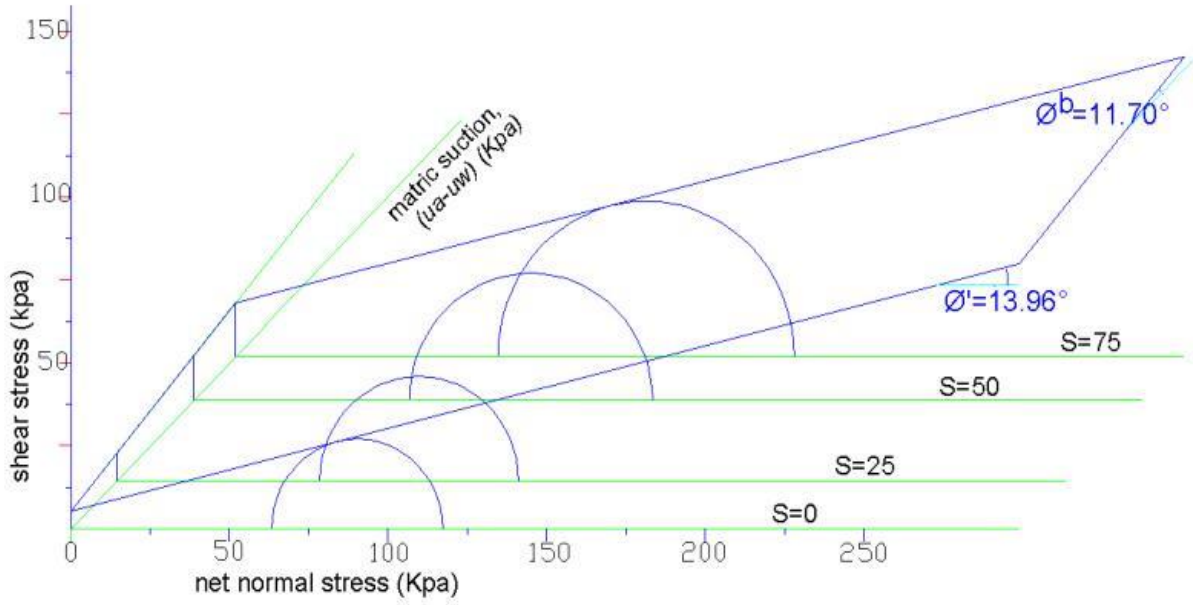

Figure 4.2 Failure envelopes for unsaturated soil from CMC area

Zhan and Ng (2006) presented results of contribution of suction to shear strength for expansive clays from china in compacted and natural specimens (figure 4.3). They also show the variation of ϕ^b angle with suction in figure 4.4.

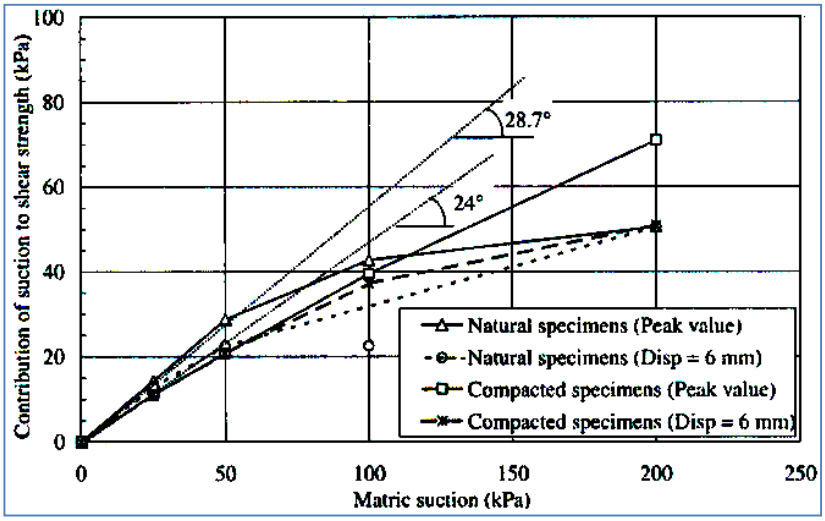

Figure 4.3 Contribution of suction to shear strength for natural and compacted specimens (Zhan and Ng, 2006).

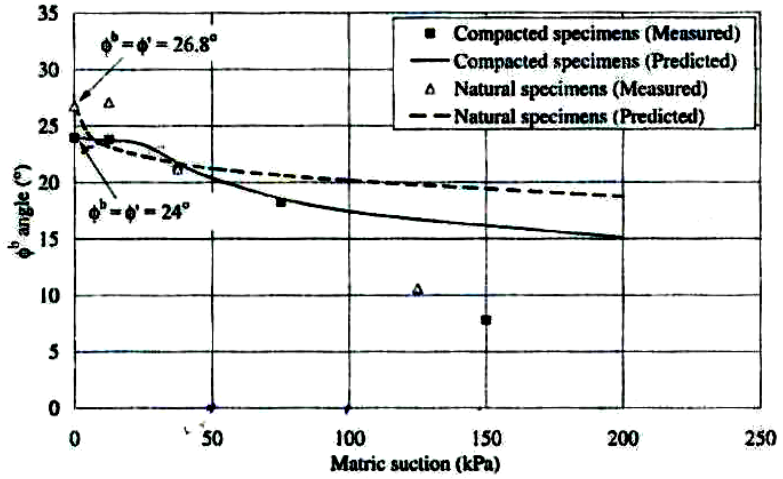

Figure 4.4 Variations of ϕ^b angles with matric suction for natural and compacted specimens (Zhan and Ng, 2006).

The soils from Bole and CMC area is compared with the results obtained from Zhan and Ng (2006) for the natural specimen. From figure 4.5 and figure 4.6, we can see that the result of Zhan and Ng soil samples is higher than that of Bole and CMC area soils. This is because of the difference in mineralogical compositions of the soils and test methods. But the trend for the

suction to shear strength curve is similar at low matric suction. Figure 4.5 show contribution of matric suction to shear strength of the soil samples. The data points were obtained by taking the shear strength measured at zero suction as a reference datum. Figure 4.6 also show that the variation of the ϕ^b angle with suction for both CMC and Bole area soils together with Zhan and Ng natural soil samples.

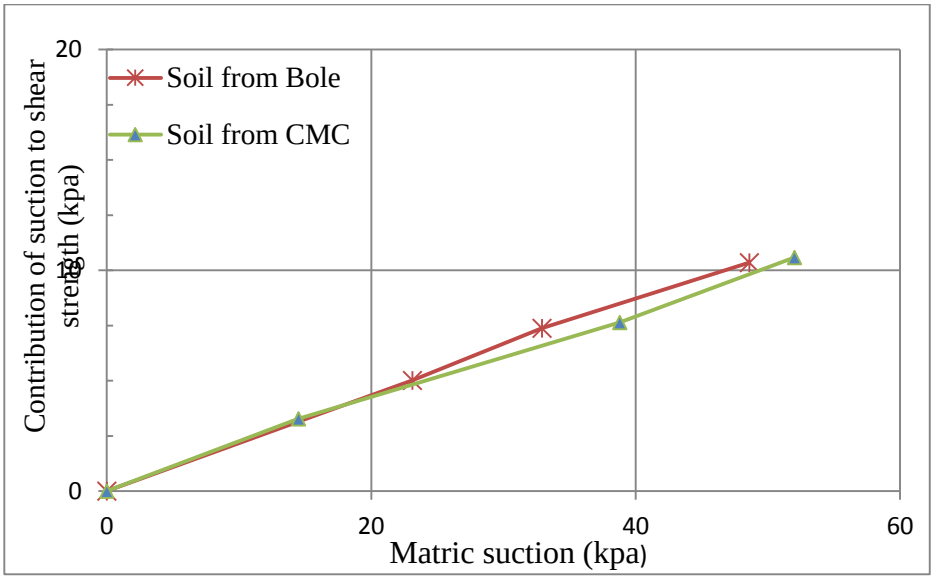

Figure 4.5 Contribution of suction to shear strength for Bole and CMC area soils.

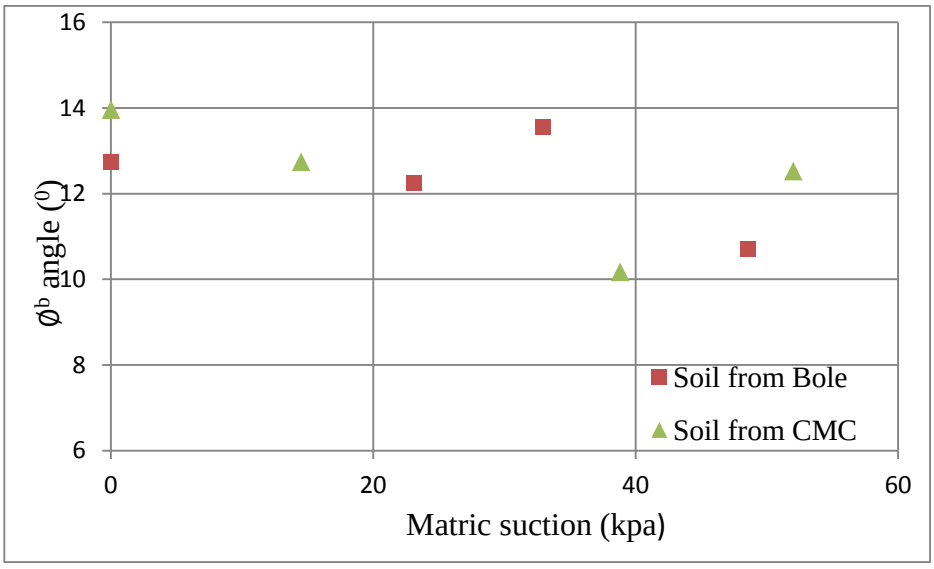

Figure 4.6 Variations of ϕ^b angles with matric suction for Bole and CMC area soils.

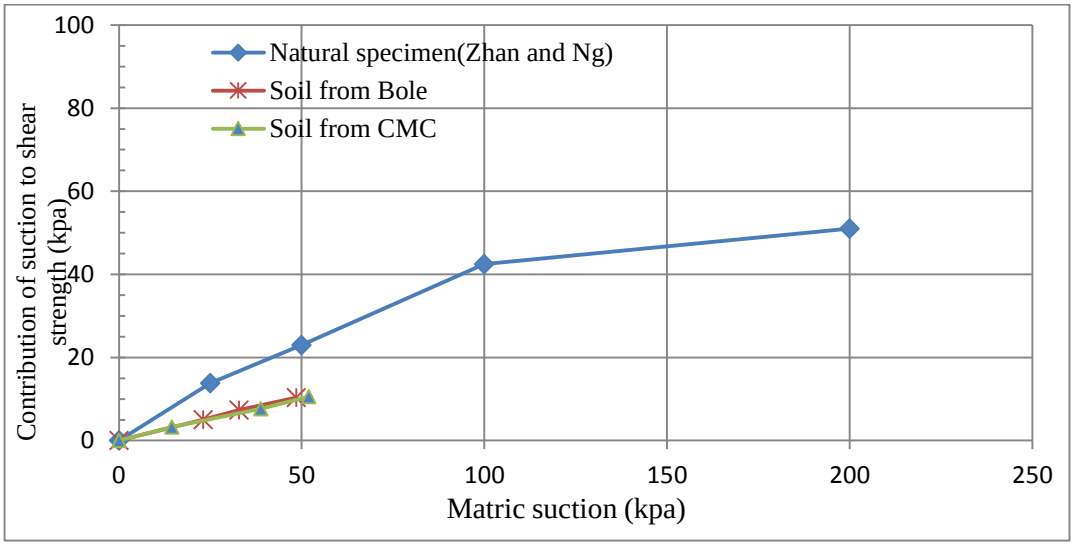

Figure 4.7 Contribution of suction to shear strength for Bole and CMC area soils together with natural specimens of Zhan and Ng (2006).

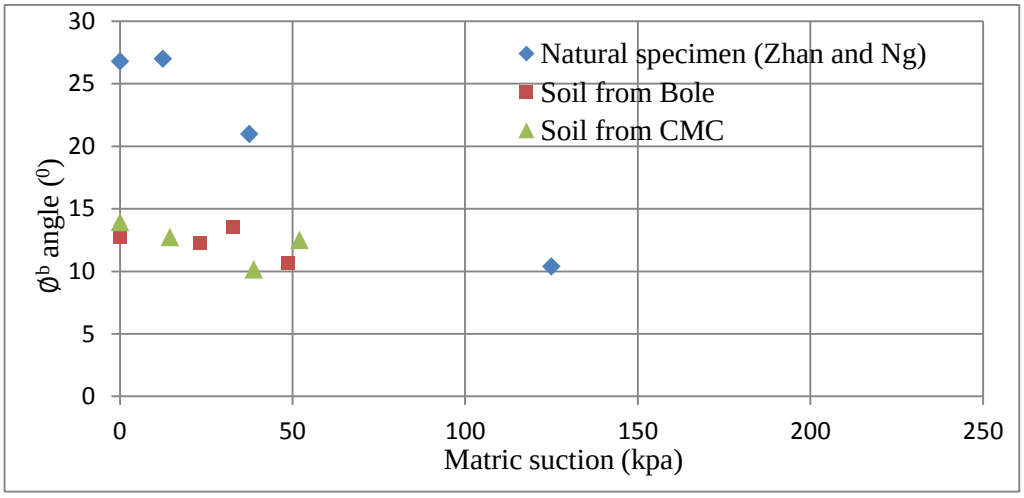

Figure 4.8 Variations of ϕ^b angles with matric suction for Bole and CMC area soils together with natural specimens of Zhan and Ng (2006).

Chapter 5 - Conclusion and recommendation

5.1 Conclusion

From the consolidated undrained triaxial test performed on expansive soils of Bole area and CMC area for unsaturated soil case the results obtained, it can be concluded that,

1. For Bole area expansive soils when matric suction of the soil increases from 0kpa to 75kpa, the value of the cohesion intercept, ***c'***, of the soil increases from 7.32 kpa to 17.67kpa for the effective consolidation of 250kpa. Similarly, for the CMC area soils the value of the cohesion intercept, ***c'***, increases from 5.39kpa to 15.97kpa for effective consolidation of 150kpa and matric suction range of 0kpa to 75kpa.
2. For Bole area expansive soils, the value of the angle ϕ^b and ϕ' are 12.05° and 12.74° respectively**.** Similarly, for the CMC area soils the value of the ϕ^b and ϕ' are 11.70° and 13.96° respectively**.** It is clearly shown that the angle ϕ^b is less than angle ϕ' for both area soils**.**
3. For Bole area expansive soils when matric suction of the soil increases from 0kpa to 75kpa, the deviator stress of the soil increases from 90.65kpa to 130.08kpa for the effective consolidation of 250kpa. Similarly, for the CMC area soils the deviator stress increases from 54.03kpa to 93.41kpa for effective consolidation of 150kpa and matric suction range of 0kpa to 75kpa.
4. As the matric suction of the soil increases, the shear strength of the soil increases nonlinearly for the applied matric suction ranges (i.e., 0kpa to 75kpa).

5.2 Recommendation

Further detail investigation required to be carried out by taking more number of samples and conducting the test on higher matric suction to see the effect.

List of References

American Association of State Highway and Transportation Officials, (2006). AASHTO Materials, Part I, Specifications, Washington, D.C.

Arora, K.R. (2000). *Soil Mechanics and Foundation Engineering*. Delhi, India.

ASTM (2004). *Standard Test Method for soil and rock*. Annual Book of ASTM Standards, Philadelphia, U.S.A.

Ayenew, Z. (2004). *Investigation into shear strength characteristics of Expansive soil of Ethiopia*. Msc Thesis, Addis Ababa University Technology Faculty, Addis Ababa, Ethiopia.

Bishop, A.W. and Henkel D.J. (1992). *The Measurement of Soil Properties in the Triaxial Test.* Edward Arnold, London.

Blight, G. E. (1997). *Mechanics of Residual Soils*. A.A Balkema, Rotterdam, Netherlands.

Bowles, J. E. (1998). *Foundation analysis and design*. The McGraw-Hill Companies, New York.

Bowles, J. E. (1984). *Physical and Geo-Technical properties of soils*. The McGraw-Hill Companies, New York.

British Standards Institution. (1990). *British standard methods of test for soils for civil engineering purposes*. Part 8. British Standards Institution, London.

Budhu, M. (2000). *Soil Mechanics & Foundations*. Wiley & Sons, New York.

Chen, F.H. (1975). *Foundations on Expansive Soils*. Elsevier Science Publishers, Amsterdam.

Daniel, T. (2003). *Examining the swelling pressure of Addis Ababa Expansive soil*. Msc Thesis, Addis Ababa University Technology Faculty, Addis Ababa, Ethiopia.

Fredlund, D.G. and Rahardjo, H. (1993). *Soil Mechanics for Unsaturated Soils*. John Wiley & Sons Inc. New York.

Fredlund, D.G., and Xing, A. (1994). Equations for the soil water characteristic curve. *Canadian Geotechnical Journal* 31(3): pp. 521-532.

Fredlund, M.D., Wilson, G.W. and Fredlund, D.G. (2002). Use of grain-size distribution for the estimation of the soil-water characteristic curve. *Canadian Geotechnical Journal* 39(5): pp. 1103-1117.

Fredlund, M.D., Wilson, G.W., and Fredlund, D.G. (1997). Prediction of the Soil-Water Characteristic Curve from the Grain-Size Distribution Curve., *Proceedings of the 3rd Symposium on Unsaturated soil*, Rio dejaneiro Brazil, April 20 -22, pp. 13-23.

Fredlund, M. D., Wilson, G.W., and Fredlund, D.G. (1995), A Knowledge-based system for Unsaturated Soils., *Proceedings of the Canadian Society of Civil Engineering Conference*, August Montreal Quebec.

Grim, R.E. (1962). *Applied Clay Mineralogy*, McGraw-Hill, New York.

Hilf, J.W. (1956). *An Investigation of Pore-Water Pressure in Compacted Cohesive Soils*. PhD dissertation, Tech. Memo. No. 654, U.S. Dept. of the Interior, Bureau of Reclamation, Design and Construction Div., Denver, CO, p. 654.

Lambe, T.W. and Whitman, R.V. (1979). *Soil Mechanics*. John Wiley and Sons, New York.

Legesse, M. (2004). *Investigating Index Property of Expansive Soil of Ethiopia*. Msc Thesis, Addis Ababa University Technology Faculty, Addis Ababa, Ethiopia.

Murthy, V.N.S. (2003). *Geotechnical Engineering: Principles and Practices of Soil Mechanics and Foundation Engineering*. Marcel Dekker, Inc., 270 Madison Avenue, Newyork.

Nelson, J.D. and Miller, D.J. (1992). *Expansive Soils: Problems and Practice in Foundation and Pavement Engineering*. New York: Wiley Interscience.

Ng, C. W. W. and Menizies, B. (2007). *Advanced unsaturated soil Mechanics and Engineering.* Taylor &Francis Group, London and New York.

Teferra, A. and Leikun, M. (1999). *Soil Mechanics*. Addis Ababa Unversity Press, Addis Ababa.

Terzaghi, K. (1936). *The shear resistance of saturated soils. Proc. 1st Int.Conf. Soil Mech. & Fdn. Engrg.*, Cambridge, Mass., Harvard University, (1), 54–56.

Terzaghi, K. (1943). *Theoretical Soil Mechanics*. John Wiley & Sons, Inc.

Zhan, T. L. T. and Ng, C. W. W. (2006). Shear strength characteristics of an unsaturated expansive clay, *Canadian Geotechnical Journal*, Vol. 43, 7, pp. 751-763.

Appendix

Appendix-A

A.1 Triaxial Tests On Unsaturated Soils

A.1.1 Consolidated drained test

The consolidated drained or CD test refers to a test condition where the soil specimen is consolidated first and then sheared under drained condition for both pore air and pore water phases. The soil specimen is consolidated to a stress state representative of what is likely to be encountered in the field or in the design. The soil is generally consolidated under an isotropic confining pressure of σ_3, while the pore air and the pore water pressures are controlled at pressures of u_a and u_w respectively. The pore air and pore water pressures can be controlled at positive values in order to establish a matric suction greater than 1 atm. without cavitation in the pore-water measuring system. This is referred to as axis translation technique, which forms the basis for laboratory testing of unsaturated soils with high matric suction with the help of specially designed high air entry disk, which allows only the passage of water (Freduland 1993). At the end of consolidation process, the soil specimen has a net confining pressure of (σ_3-u_a) and a matric suction of (u_a-u_w) (Freduland 1993).

During the shearing process, the soil specimen is compressed in the axial direction by applying a deviator stress [i.e $(\sigma_1-\sigma_3)$]. During shear the drainage valves for both pore air and pore water remain open (under drained conditions) (Freduland 1993). The pore air and the pore water pressures are controlled at constant pressures (their pressures at the end of consolidation). The deviator stress is applied slowly in order to prevent the development of excess pore air or pore water pressure in the soil (Freduland 1993). Using the deviator stress and the matric suction at failure the Mohr circle will be drawn and the required parameters determined.

Typical stress path followed during consolidated drained tests under constant matric suction are illustrated in figure A-1. The tests are performed on several specimens at various net confining pressures. For instance stress point *A* represents the stress state at the end of consolidation when the soil specimen has a net confining pressure of (σ_3-u_a) and a matric suction of (u_a-u_w). As the soil is compressed during shear, the stress point moves from point *A* to point *B* along the stress path *AB*. Stress point *B* represents the stress state at the condition of failure. When moving from stress point *A* to point *B*, the Mohr circle diameter or deviator stress increases until the failure condition is reached at stress point *B*. However, the net confining pressure and the matric suction

remain constant throughout the stress path *AB.* The line drawn tangent to the Mohr circles at failure (i.e through stress points *C*, C_1 and C_2) represents the failure envelope corresponding to the matric suction used in the tests. The failure envelope has a slope angle of ϕ', which is known as the angle of internal friction, with respect to the (σ_3-u_a) axis. The friction angle appears to be essentially equal to the effective angle of internal friction obtained from shear strength tests on saturated soils. The cohesion intercepts obtained at various matric suctions can be joined to give the angle, ϕ^b (Fredlund, 1993).

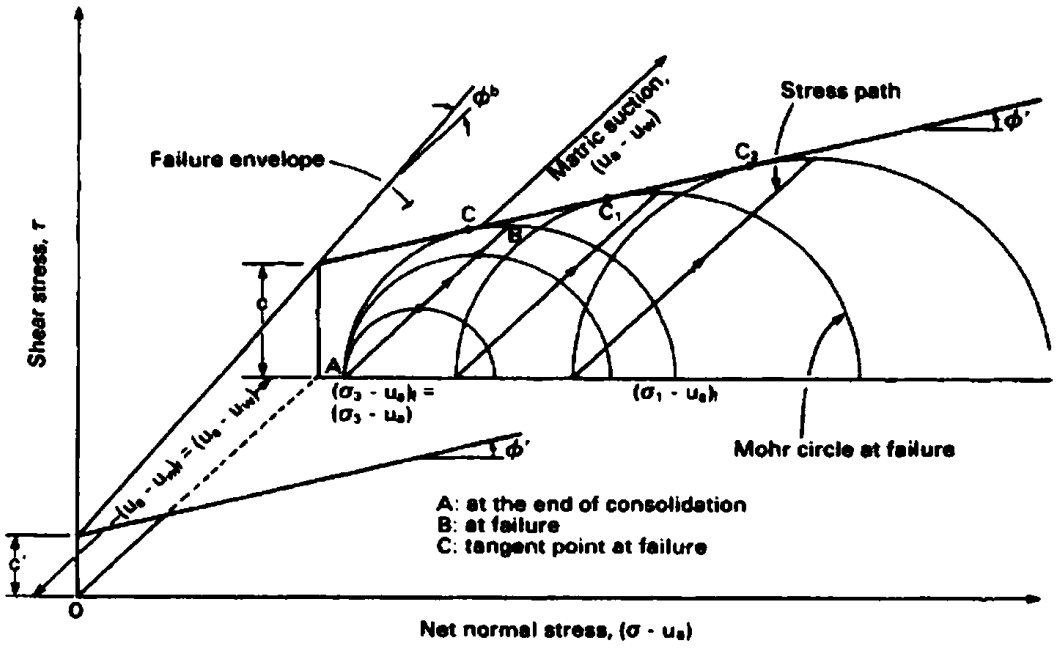

(a)

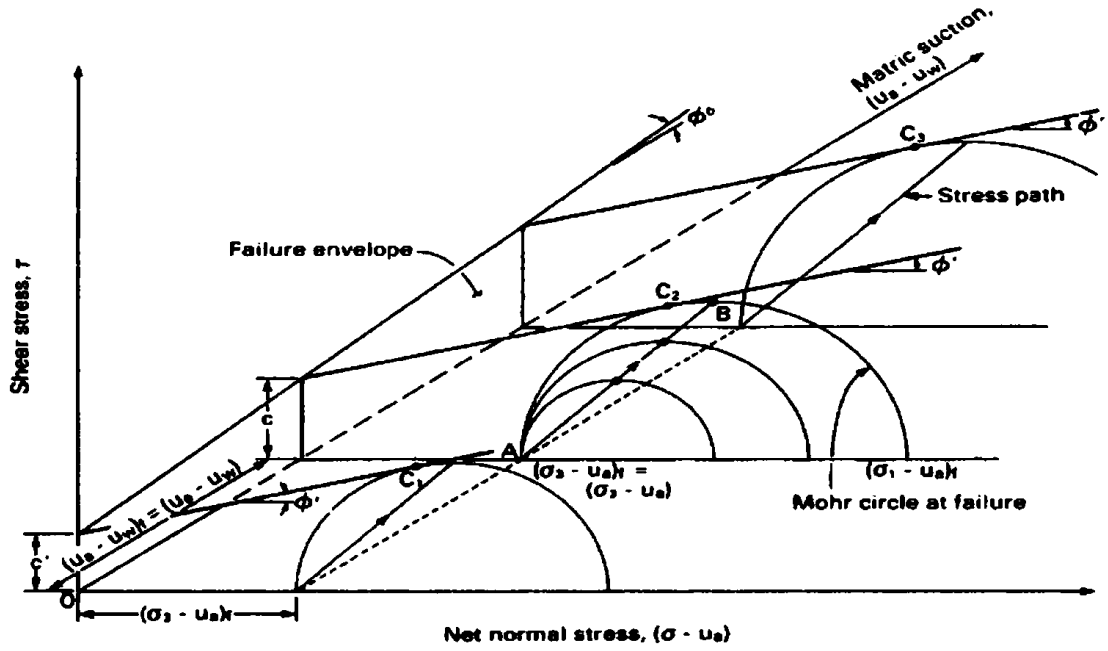

(b)

Figure A- 1. Stress path followed during a consolidated drained test (a).at various net confining pressures and constant matric suction (b).at various matric suction and constant confining pressures (Freduland 1993).

A.1.2 Constant water content test

For the constant water content test or CW test, the specimen is first consolidated and then sheared, with the pore air phase allowed to drain while the pore water phase is in an undrained mode (Freduland 1993). The consolidation procedure is similar to that of the consolidated drained test. At the end of consolidation, the soil will have a net confining pressure (σ_3-u_a) and a matric suction of (u_a-u_w). The specimen is sheared by increasing the deviator stress $(\sigma_3-\sigma_1)$ until failure is reached. During shear the drainage valve for the pore air remains open (under drained conditions), while the drainage valve for the pore water is closed (under undrained conditions). In this test the net confining pressure ,(σ_3-u_a), remains constant trough out the test, while the matric suction, (u_a-u_w), changes due to the increase in the pore water pressure during the application of the deviator stress.(i.e ,$(\sigma_3-u_a)_f = (\sigma_3-u_a)$ and $(u_a-u_w)_f = (u_a-u_w)-\Delta u_w$)) (Freduland 1993).

A hypothetical stress path that may be followed by the soil specimen during a constant water content test is shown in Figure A-2. Stress point *A* represents the stress state at the end of

consolidation where the soil specimen has a net confining pressure of (σ_3-u_a) and a matric suction of (u_a-u_w). As the soil is compressed during shear, the stress point is assumed to move from point *A* to point *B* along stress path *AB*. Stress point *B* represents the stress state at failure. The net confining pressure remains constant at (σ_3-u_a) along the stress path *AB* since the pore air pressure is maintained at the pressure used during consolidation. The pore water pressure is assumed to increase continuously during shear. This results in a reduction in the matric suction [i.e. $(u_a-u_w)_f < (u_a-u_w)$]. The failure envelope sloping at an angle of ϕ' can be drawn tangent to the Mohr circle at failure, at stress point *C*. The failure envelope intersects the shear strength verses matric suction plane at cohesion intercept, *c*. The cohesion intercepts obtained at various matric suctions can be joined to give the ϕ^b values (Fredlund 1993).

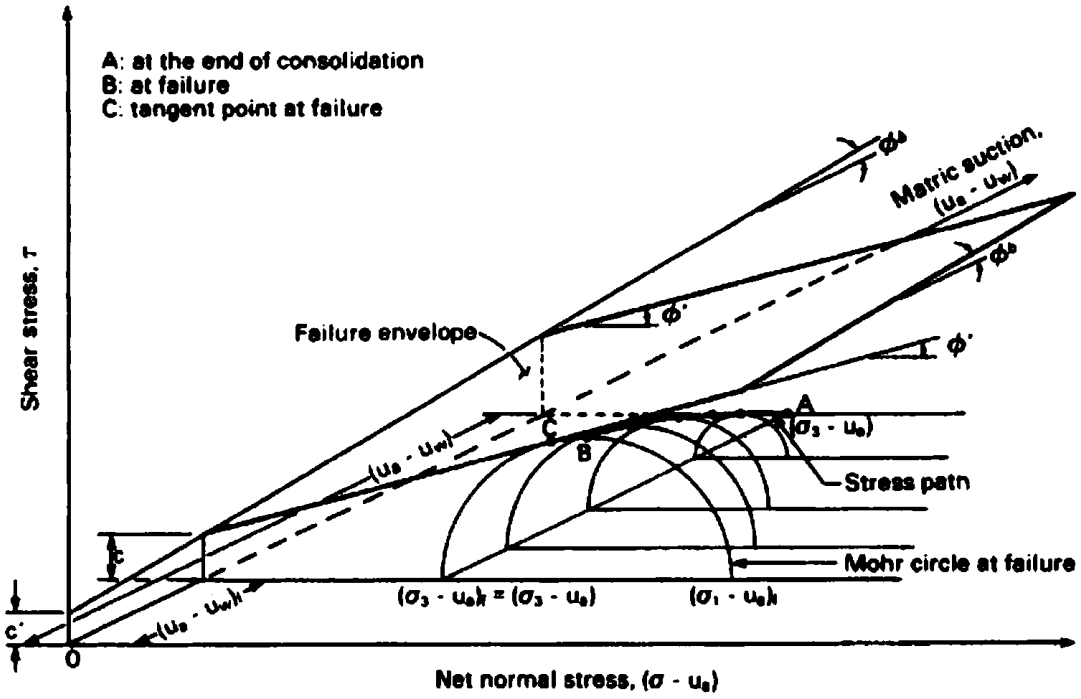

Figure A- 2. Stress path followed during constant water content test (Fredlund 1993).

A.1.3 Undrained test

The pore air and pore water are not allowed to drain in the undrained test. This applies both when the confining pressure and the deviator stress are applied to the soil specimen. The excess pore air and pore water pressure developed during the application of the confining pressure can be related to the isotropic confining pressure by use of *B*-value pore pressure parameter

(Fredlund, 1993). Although the excess pore pressures built up during the application of confining pressure are not allowed to dissipate, the volume of soils specimen may change due to the compression of pore air. The soil has a net confining pressure (σ_3-u_a), and matric suction, $(u_a - u_w)$, after the application of the confining pressure (Fredlund, 1993).

The soil specimen is sheared by applying an axial stress $(\sigma_1-\sigma_3)$ until failure is reached. Undrained loading during shear causes further development of excess pore air and pore water pressures. The excess pore pressure parameters for triaxial loading condition can be related to the deviator stress by the *D*-value pore water pressure Parameter. Generally the pore pressures are not measured during shear. Therefore, the undrained test results are commonly used in conjunction with a total stress formulation of a problem. Here, the shear strength is related to the total stress without knowledge of pore pressure at failure (Fredlund, 1993).

The net confining pressure, (σ_3-u_a), and the matric suction, (u_a-u_w), vary throughout the shearing process. However, the stress state variables during shear and at failure are unknown since the pore pressures are not measured. Only the total confining pressure and the deviator stress, $(\sigma_1-\sigma_3)$, are measured values in the test (Fredlund, 1993).

A hypothetical stress path that may be followed by the soil specimen during undrained test is illustrated in Figure A-3. In the illustration, four identical specimens are considered that are initially confined at four different confining pressures. These are represented by stress points *A*, A_1, A_2, and A_3, Where σ_3 at $A < \sigma_3$ at $A_1 < \sigma_3$ at $A_2 < \sigma_3$ at A_3. The application of the total confining pressure under undrained conditions results in the compression of the pore fluids and the development of excess pore air and pore water pressures. The pore pressure increases in unsaturated soils are always less than the total stress increment applied σ_3 (Fredlund, 1993). This is in keeping with *B*-value pore pressure parameters which must always be less than 1 for unsaturated soils. Therefore, a higher total confining pressure results in a higher net confining pressure (i.e.(σ_3-u_a) at $A< (\sigma_3-u_a)$ at $A_1 < (\sigma_3-u_a)$ at $A_2 < (\sigma_3-u_a)$ at A_3) and lower matric suction (i.e.(u_a-u_w) at $A > (u_a-u_w)$ at $A_1>(u_a-u_w)$at $A_2>(u_a-u_w)$ at A_3). In other words, the four identical soil specimens are brought to four initial stress states, represented by stress points *A*, A_1, A_2, and A_3 (Figure A-3). As the soil is sheared in undrained loading, the pore fluids are further compressed and the pore pressures may further increase. The stress point moves from point *A* to point *B*

along the stress path *AB*. The net confining pressure and and the matric suction decrease when going from stress point *A* to stress point *B*. Stress point *B* represents the stress state of the soil at failure. Similar stress paths are followed by other specimens at stress points A_1, A_2, A_3 along stress paths of A_1B_1, A_2B_2, and A_3B_3 (Fredlund, 1993).

Figure A-3 indicates that an increase in the diameter of the Mohr circle at failure as the initial total confining pressure increases. In other words, the shear strength of the soil increases with increasing initial total confining pressure, although the initial matric suction decreases. This occurs because the rate of shear strength increase caused by an increase in confining pressure is greater than the reduction in shear strength caused by a decrease in matric suction (Fredlund, 1993).

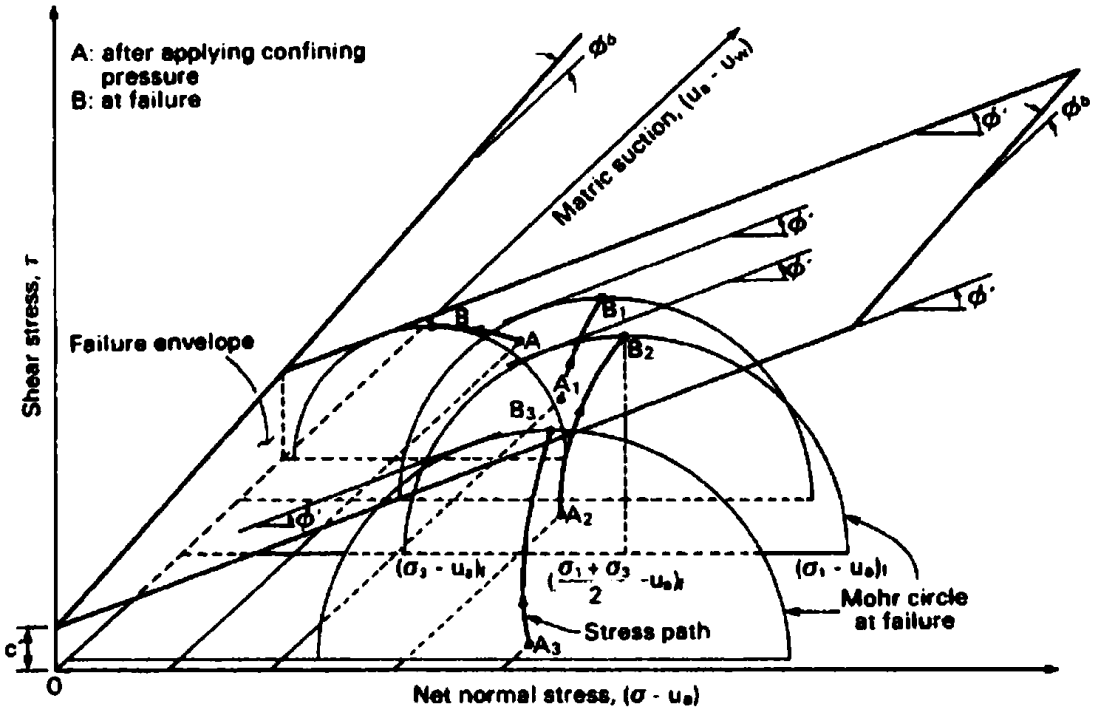

Figure A- 3. stress paths followed during undrained tests (Fredlund, 1993).

A.1.4 Unconfined compression test

The unconfined compression Test or UC is special case of the undrained test. No confining Pressure is applied to the soil specimen throughout the test. The test can be performed by applying a load in a simple loading frame. At the start of the test, the unsaturated soil Specimen

has negative pore water pressure, and pore air pressure is assumed to be atmospheric. The soil matric suction (u_a-u_w) is therefore numerically equal to pore water pressure (Fredlund, 1993).

The soil specimen is sheared by applying an axial load until failure is reached. The Deviator stress, $(\sigma_1-\sigma_3)$, is equal to the major principal stress, σ_1, and the minor principal stress, σ_3, is equal to zero as there is no any confining pressure. The compressive load is applied quickly in order to maintain undrained conditions. This should apply to both pore air and pore water phases. The pore air and pore water pressures are not measured during Compression. The excess pore pressure developed during unconfined compression Test can be theoretically related to the major principal stress through use of the *D*-value or *B*-value pore pressure parameter. Figure A-4 shows two possible stress paths that may be followed in unsaturated soil specimen during the unconfined compression test. The initial stress state is represented by stress point A where the soil has a zero net confining pressure. During undrained compression, the matric suction can increase, decrease, or remain constant depending up on the *A* parameter of the soil. Generally, the matric suction decreases during an undrained compression test and the stress state in the soil will move forward from point *A* to point *B* along the stress path *AB*. The stress state of the soil at failure is represented by point *B*. The pore air pressure is assumed to increase slightly during compression. This causes the net confining pressure to decrease along the stress path *AB* to a negative Value. The matric suction at failure is less than the initial matric suction at *A* (Fredlund, 1993).

In case of constant matric suction during compression, the stress path lies on the plane of constant matric suction (i.e. stress path AB_1 of figure A-4). For the case of increase in matric suction during compression, the stress state in the soil will move backwards from point *A* to a point (or plane) somewhere behind point A (Fredlund, 1993).

The deviator stress at failure is usually referred as the unconfined compressive strength. The unconfined compressive strength is commonly taken as being equal to twice the undrained shear strength. As the confining pressure increases, the undrained shear strength for unsaturated soils also increases. As a result, the compressive strength values may not be satisfactory in approximating the undrained shear strength (Fredlund, 1993)..

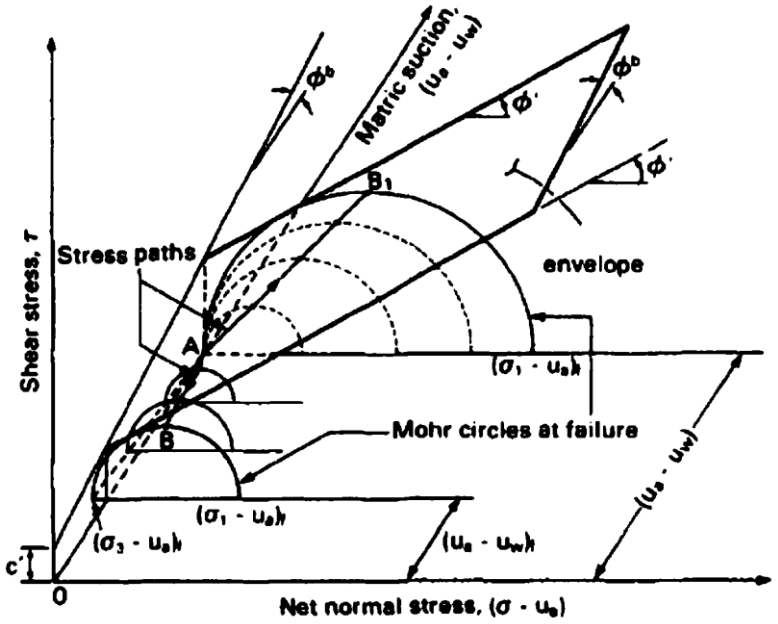

Figure A- 4. possible stress paths followed during an unconfined compression test (Fredlund, 1993).

A.2 Direct shear test

A direct shear test apparatus basically consists of a split box, with a top and bottom portion. The test is generally performed using a consolidated drained procedure. A soil specimen is placed in the direct shear box and consolidated under vertical normal stress, σ. During consolidation, the pore air and pore water pressures must be controlled at selected pressures. The axis-translation technique can be used to impose a matric suction greater than 1 atm. The direct shear test can be conducted in an air-pressurized chamber in order to elevate the pore air pressure to a magnitude above atmospheric pressure (i.e. 101.3 kPa). The pore water pressure can be controlled below the soil specimen using a high air-entry disk. At the end of the consolidation process, the soil specimen has a net vertical normal stress of $(\sigma_n - u_a)$ and a matric suction of $(u_a - u_w)$. Shearing is achieved by horizontally displacing the top half of the direct shear box relative to the bottom half. The soil specimen is sheared along a horizontal plane between the top and bottom halves of the direct shear box. The horizontal load required to shear the specimen, divided by the nominal area of the specimen, gives the shear stress on the shear plane. During shear, the pore air and pore water pressures are controlled at constant values. Shear stress is increased until the soil specimen fails. The failure plane has a shear stress designated as τ_{ff} corresponding to a net

vertical normal stress of $(\sigma_f\text{-}u_a)_f$ [i.e. equal to $(\sigma\text{-}u_a)$ at failure] and a matric suction of $(u_a\text{-}u_w)_f$ [i.e. equal to $(u_a\text{-}u_w)$ at failure] (Fredlund, 1993).

The failure envelope can be obtained from the results of direct shear tests without constructing the Mohr-circles. The shear stress at failure, τ_{ff}, is plotted as the ordinate, and $(\sigma_f\text{-}u_a)_f$ and $(u_a\text{-}u_w)_f$ are plotted as the abscissas to give a point on the failure envelope (Figure A-5). A line joining points of equal magnitude of $(\sigma_f\text{-}u_a)_f$ determines the ϕ^b angle (e.g., line joining points *A*, *B* and *C* in Figure A-5). Similarly, a line can be drawn through the points of equal $(u_a\text{-}u_w)_f$ to give the angle of internal friction ϕ' (e.g., a line drawn through points A_1, A_2 and *A* in Figure A-5) (Fredlund, 1993).

The direct shear test is particularly useful for testing unsaturated soils due to the short drainage path in the specimen. The low coefficient of permeability of unsaturated soils results in 'times to failure' in triaxial tests, which can be excessive. Other problems associated with testing unsaturated soils in a direct shear apparatus are similar to those common to saturated soils (e.g. stress concentrations, definition of the failure plane, and the rotation of principal stresses) (Fredlund, 1993).

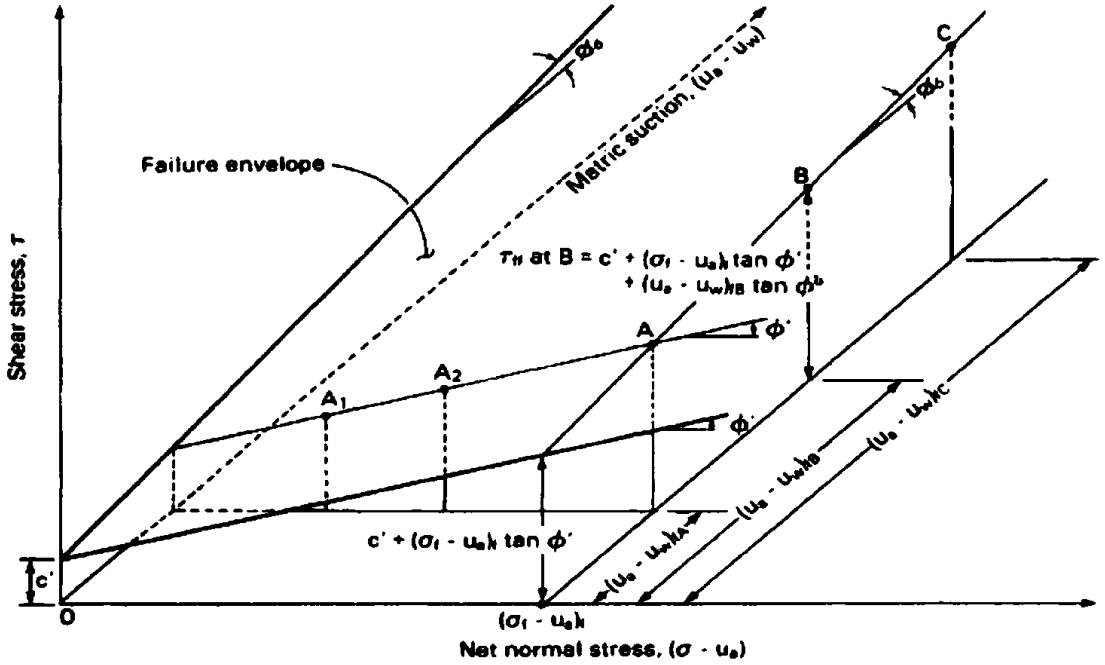

Figure A- 5 Extended Mohr-coulomb failure envelope established from direct shear test results (Fredlund, 1993).

Table A- 1. Data used for plastic and liquid limit analysis for soils from Bole area

	Liquid Limit			Plastic Limit	
Trial No	1	2	3	1	2
Container No	A18	A29	C35	65	D34
Mass of container, g	23.52	23.37	23.41	12.47	12.98
Mass of container + Wet soil, g	48.76	49.59	50.93	22.15	22.60
Mass of container + Dry soil, g	36.25	36.50	37.15	19.21	19.66
Mass of water, g	12.51	13.09	13.78	2.94	2.94
Mass of dry soil, g	12.73	13.13	13.74	6.74	6.68
Water content, %	98.27	99.70	100.29	43.62	44.01
No of blows	34	26	22	------	------

Liquid Limit, % = 99.75 Plastic Limit, % = 43.82 PI, %= 55.93

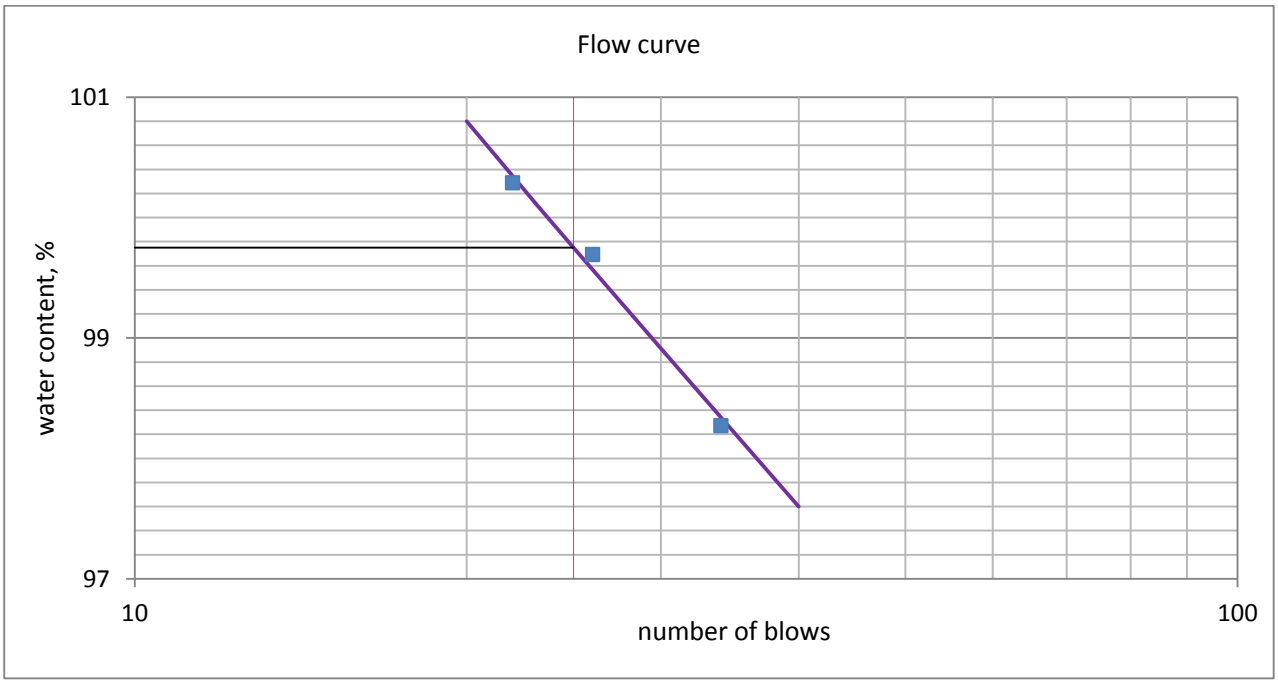

Figure A- 6 Flow curve for soils from Bole area

Table A- 2 Data used for plastic and liquid limit analysis for soil from CMC area

	Liquid Limit			Plastic Limit	
Trial No	1	2	3	1	2
Container No	A13	C15	98	76	D34
Mass of container, g	23.37	23.39	23.01	12.73	12.78
Mass of container + Wet soil, g	51.45	50.16	44.46	19.56	19.96
Mass of container + Dry soil, g	39.30	38.51	35.00	17.47	17.75
Mass of water, g	12.15	11.65	9.46	2.09	2.21
Mass of dry soil, g	15.93	15.12	11.99	4.74	4.97
Water content, %	76.27	77.05	78.90	44.09	44.47
No of blows	33	28	19	------	------

Liquid limit,% = 77.60 Plastic limit,% = 44.30 PI,% = 33.30

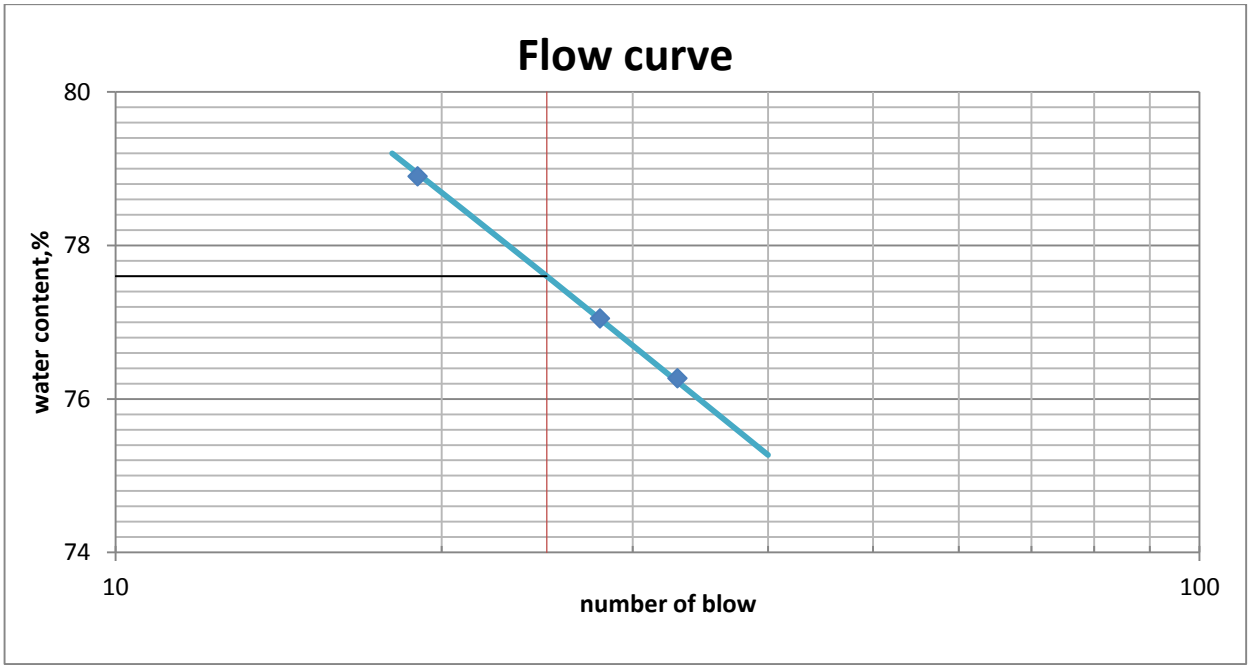

Figure A- 7 Flow curve for soil from CMC area

Table A- 3 Hydrometer analysis for soil from Bole area

Specific Gravity of soil 2.63 Test Temperature, deg.c 20

Elapsed Time (min)	Actual Hydrometer Reading	Temp. ^{0}c	Corrected Hydrometer Reading	Effective Depth (cm)	Coeffici ent, K	Grain Size (mm)	% Finer
2	49.0000	20.0	42.0000	9.40	0.01374	0.0298	95.53
5	48.0000	20.0	41.0000	9.60	0.01374	0.0190	93.25
15	47.5000	20.0	40.5000	9.65	0.01374	0.0110	92.12
30	46.5000	20.0	39.5000	9.80	0.01374	0.0079	89.84
60	45.0000	20.0	38.0000	10.10	0.01374	0.0056	86.43
250	44.0000	21.0	37.5000	10.15	0.01349	0.0027	85.29
1440	43.0000	20.0	36.0000	10.40	0.01374	0.0012	81.88

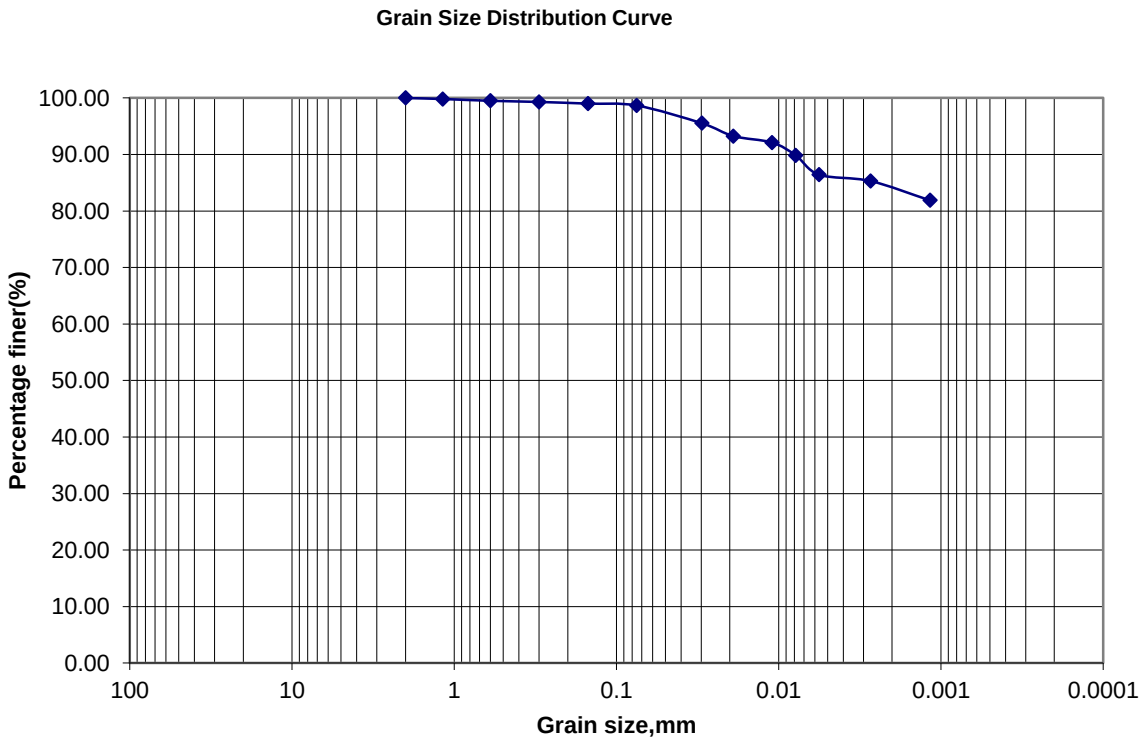

Figure A- 8 Grain size curve for soil from Bole area

Table A- 4 Hydrometer analysis for soil from CMC area

Specific Gravity of soil 2.65 Test Temperature, deg.c 20

Elapsed Time (min)	Actual Hydrometer Reading	Temp. ^{0}c	Corrected Hydrometer Reading	Effective Depth (cm)	Coefficient, K	Grain Size (mm)	% Finer
2	56.0000	20.0	49.0000	8.30	0.01365	0.0278	89.48
5	55.5000	20.0	48.5000	8.35	0.01365	0.0176	88.57
15	53.5000	20.0	46.5000	8.70	0.01365	0.0104	84.92
30	51.5000	20.0	44.5000	9.00	0.01365	0.0075	81.26
60	50.0000	20.0	43.0000	9.20	0.01365	0.0053	78.52
250	47.5000	21.0	41.0000	9.60	0.01348	0.0026	74.87
1440	46.5000	20.0	39.5000	9.80	0.01365	0.0011	72.13

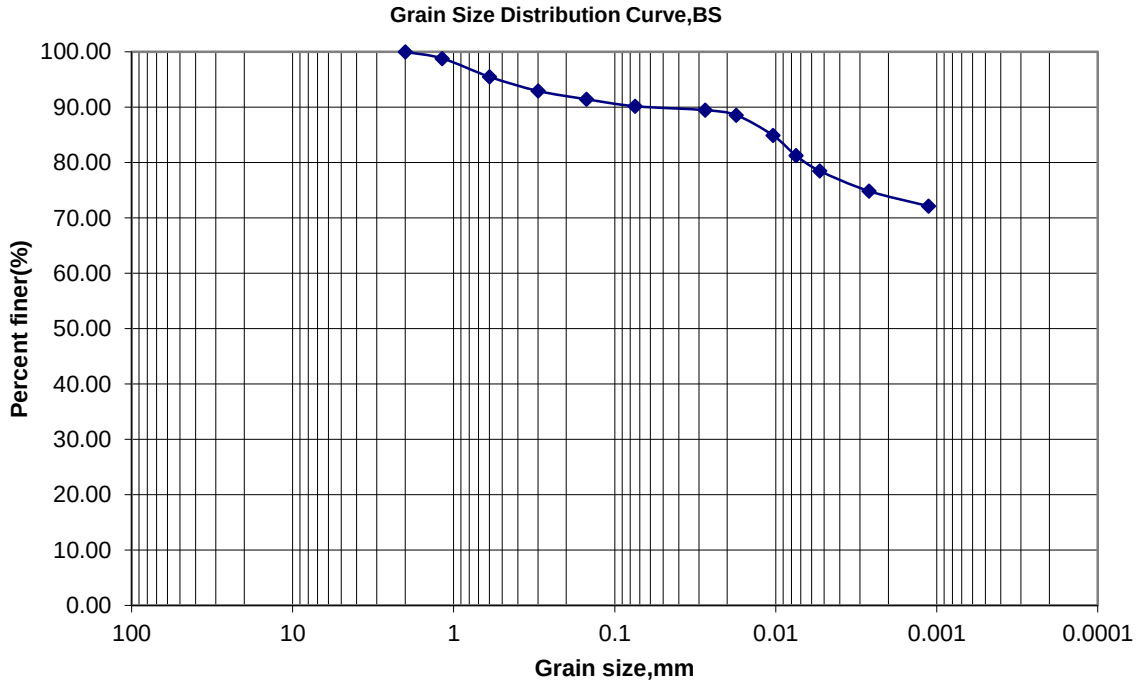

Figure A- 9 Grain size curve for soil from CMC area

Table A- 5 Natural moisture content of the samples

Sample No.	Wt of Can(gr)	Wt of wet soil & can (gr)	Wt of dry soil & can (gr)	Moisture content (%)
B-1	5.38	125.87	88.63	44.73
B-2	5.31	168.64	121.39	40.70
B-3	5.42	154.32	108.67	44.21
B-4	5.31	139.63	100.46	41.17
B-5	5.53	142.43	102.27	41.51
B-6	5.32	140.58	101.48	40.66
C-1	5.38	197.00	138.44	44.01
C-2	5.31	122.73	86.05	45.43
C-3	5.24	128.94	90.30	45.43
C-4	5.36	68.36	46.53	53.02
C-5	5.30	94.89	66.21	47.09
C-6	5.42	156.60	104.63	52.38

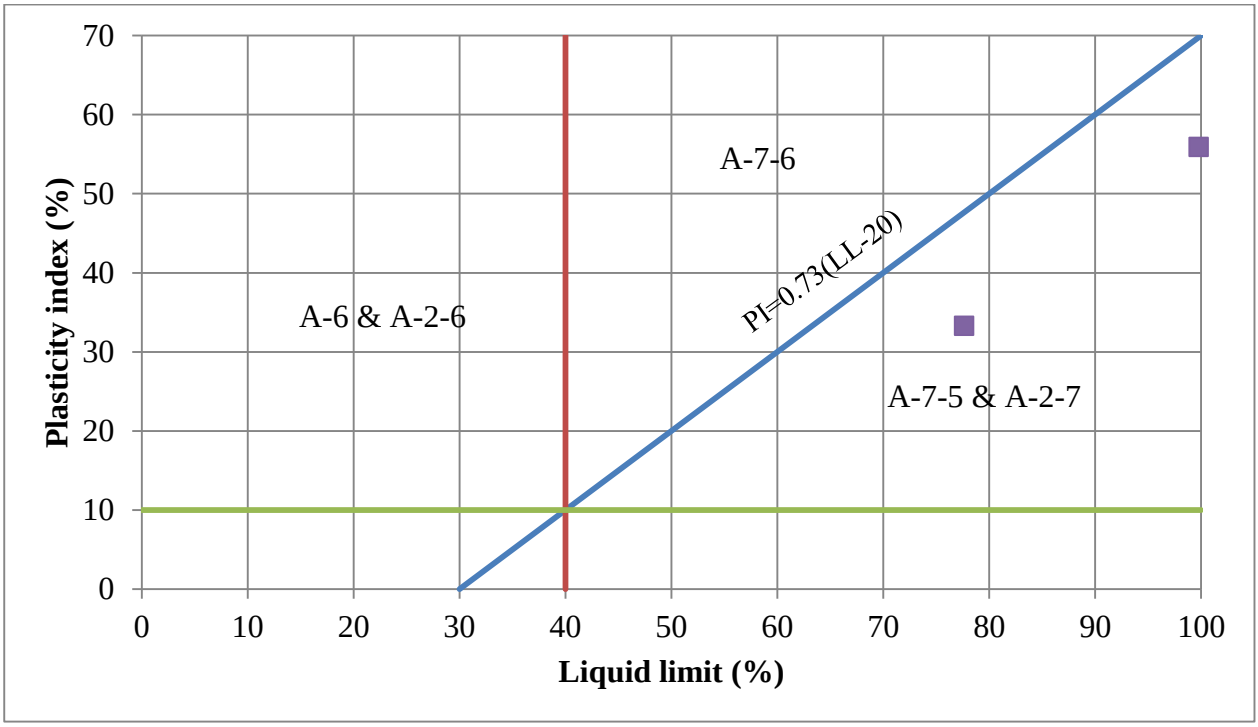

Figure A- 10 Classification of the soil of the study area according to AASHTO methods

Table A- 6 Parameters used to draw the Mohr circles for saturated soils (results obtained from the consolidated undrained test)

Site	**Sample No**	σ_3	Excess pore water Δu_w	$(\sigma_1 - \sigma_3)$	σ_1	$\sigma'_1 = \sigma_1 - \Delta u_w$	$\sigma'_3 = \sigma_3 - \Delta u_w$
CMC	C-1	150	86.70	54.03	204.03	117.33	63.30
	C-2	200	113.20	68.92	268.92	155.72	86.80
	C-3	250	140.50	87.78	337.78	197.28	109.50
Bole	B-1	150	74.10	61.36	211.36	137.26	75.90
	B-2	200	104.63	72.284	272.28	167.66	95.37
	B-3	250	122.17	90.65	340.65	218.47	127.83

Table A- 7 Parameters used to draw the Mohr circles for unsaturated soils (results obtained from the consolidated undrained test)

Site	**Sample No**	σ_3	S	Excess pore air Δu_a	Excess pore water Δu_w	$S_{(at\ failure)}$	$(\sigma_1 - \sigma_3)$	σ_1	$\sigma'_1 = \sigma_1 - \Delta u_a$	$\sigma'_3 = \sigma_3 - \Delta u_a$
CMC	C-4	150	25	86.11	96.71	14.50	62.79	212.79	126.68	63.89
	C-5	150	50	81.92	93.30	38.82	76.59	226.58	144.67	68.08
	C-6	150	75	64.33	87.50	52.03	93.41	243.41	179.08	85.67
Bole	B-4	250	25	116.81	119.33	23.08	106.21	356.21	239.40	133.19
	B-5	250	50	111.05	128.05	32.90	115.38	365.38	254.33	138.95
	B-6	250	75	98.27	124.57	48.60	130.08	380.08	281.81	151.73

Appendix-B

Figure B- 11 Extruding undisturbed soil sample from the sampling tube.

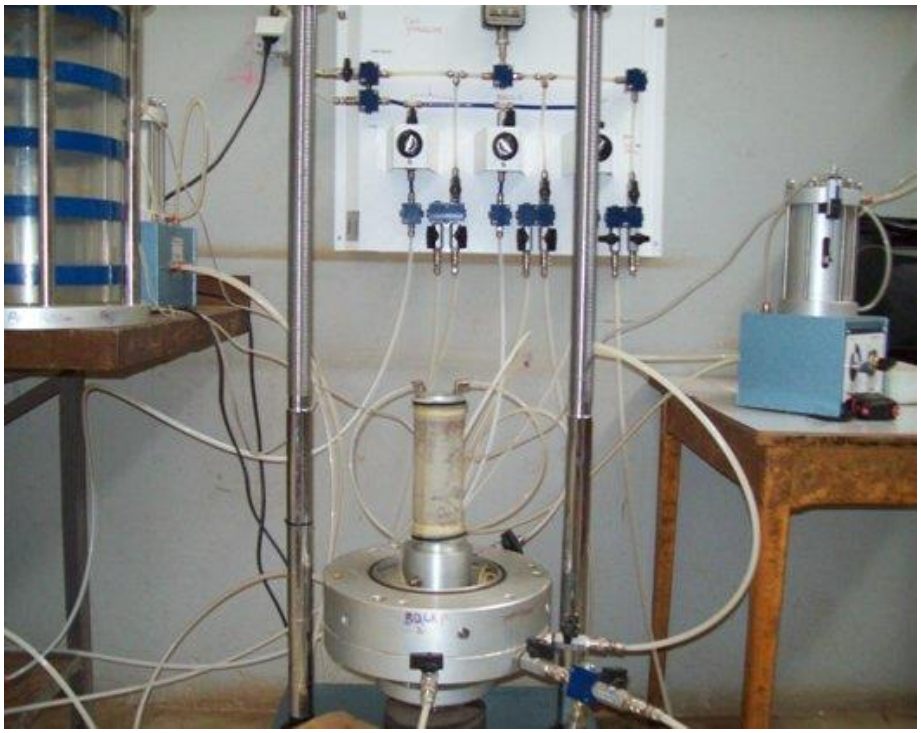

Figure B- 12 Soil sample mounted on Modified triaxial machine.

Figure B- 13 Soil sample after shearing